

NEWS AND VIEWS

A new model for circadian clock research?

Daniel Forger, Mark Drapeau, Ben Collins and Justin Blau

Department of Biology, New York University, New York, NY, USA

Molecular Systems Biology 28 June 2005; doi:10.1038/msb4100019

From a closer and purer league between...the experimental and the rational...much may be hoped. (Bacon, 1620)

Although Francis Bacon proposed the benefits of interdisciplinary science in 1620, only recently have molecular biologists and mathematicians talked with any frequency. Although no modern biologist would deny the validity of computational approaches in biology—just look at the burgeoning field of Genomics—how useful mathematical modeling will be to biologists remains debated (Lawrence, 2004; Tyson, 2004). An answer may be here with a study in this issue of MSB by Locke *et al* (2005), which highlights the advantages of being able to work effectively with models and molecules.

The study by Locke *et al* (2005) focuses on circadian rhythms, daily rhythms of behavior and physiology found in most organisms. These rhythms range from human sleep/wake cycles to leaf movements in plants. The cyclical nature and the precision of these internally driven rhythms has intrigued mathematicians and biologists alike. Yet despite working on the same questions for decades, most circadian molecular biologists have not embraced mathematical modeling. The following dialogue highlights similarities and differences in the views of a biologist (B) and a mathematician (M):

B: I don't understand how 'Math-Biology' will help my research—mathematical models seem more descriptive than predictive.

M: Well, I have an excellent paper for you to read in which the authors move freely between computer simulations and experiments. Locke *et al* (2005) used experimental data to build a model, and then tested whether this model could predict other experimental data not initially included. Their initial model had only three genes in the network and did not match the *in vivo* data—so Locke *et al* added hypothetical components to make the model more accurate. Their simulations worked so well that they were able to return to experiments and identify a strong candidate for one of the hypothetical components.

B: That does sound useful. What were they modeling?

M: The *Arabidopsis* circadian clock.

B: Oh yes, I read about that. I can guess which genes they started with: *TIMING OF CAB EXPRESSION 1 (TOC1)*, *LATE ELONGATED HYPOCOTYL (LHY)* and *CIRCADIAN CLOCK ASSOCIATED 1 (CCA1)*. Experiments have shown that TOC1 activates *LHY* and *CCA1* expression, and that *LHY* and *CCA1* proteins then feed back to inhibit *TOC1* expression and, consequently, to inhibit further *LHY* and *CCA1* expression

(Alabadi *et al*, 2001). A classical clock negative feedback loop. In fact, the clocks in *Drosophila* and mammals have two of these transcription/translation feedback loops interlocked with one another (Hardin, 2004).

M: Yes, that's right. In their paper, Locke *et al* found that the single TOC1/LHY/CCA1 loop could not explain data that they measured *in vivo*, such as weak residual 18 h rhythms in plants with both *lhy* and *cca1* mutated. So they added a second loop to the *Arabidopsis* clock, and their simulations were much more accurate.

B: But there are two loops in the *Drosophila* and mammalian circadian clocks (Hardin, 2004), so is it really a surprise to find the same in plants? That does not seem very predictive.

M: Wait: The authors' simulations predicted that RNA levels of 'Factor Y', the key player in the second loop of their model, would show two peaks of expression every day—a burst of expression at dawn, and a broader peak at dusk. Then they went back to the bench and looked at the expression profiles of a number of genes known to affect circadian gene expression but which had not yet been fitted into the molecular clock network. Since they were looking for a very brief peak of RNA at dawn, they designed their experiments to sample every hour around dawn and then less frequently over the rest of the day.

B: And?

M: They found one gene, *GIGANTEA (GI)*, whose expression paralleled the rhythms of Factor Y.

B: So is GI Factor Y?

M: Probably, because *gi* mutants have low amplitude molecular clock oscillations (Mizoguchi *et al*, 2002). It is a very strong candidate, but we will need experiments to test this.

B: Great! But how did Locke *et al* design an accurate model without knowing the abundance or half-lives of any of these proteins?

M: This is called an inverse problem in Mathematics and, rather than starting with known parameters, they have to be chosen to match experimental data. Then one runs simulations to see if the model fits experimental data. This type of parameter sampling is widespread in other areas of mathematical modeling and was used to model the mammalian circadian clock (Forger and Peskin, 2003). When I said that Locke *et al*'s one-loop model did not match the experimental data, I meant that they could not find a set of parameters that would simulate the experimental data.

B: I see. So does all of this mean that I should run a simulation before my next experiment? Not a chance!

M: Funny that you say that. This is one of the implications of Locke *et al*'s study—that simulations can help design great experiments. Remember, circadian expression profiles for much of the *Arabidopsis* genome have been available for nearly 5 years (Harmer *et al*, 2000), but the dawn peak of *GI* expression was missed because the sampling times were every four hours. I don't know if anyone would have caught this early *GI* peak unless they sampled at one hour intervals. So simulations were invaluable in this case. You know, there are models and interactive, user-friendly tools for biologists to run simulations on the Web—for example, www.amillar.org/Downloads.html, www.sbml.org or www.BioSpice.org.

B: But how would I know which model to use? It is a long time since I studied Mathematics.

M: You need to look for rigor in the model: Biological rigor—the modeler should precisely state all biological assumptions; Mathematical rigor—the modeler should describe exactly how these assumptions were converted into equations; and Numerical rigor—the modeler should justify how these equations were solved. And the model that most accurately reflects the biology may be complex. If the underlying biology is complex (many proteins, many cells, etc.), then do not expect a simple model.

B: But do you really think that this can help Biology in general? We already know about so many genes and so many pathways.

M: That is my main point. As biologists find increasing numbers of components in pathways, computer simulations will be needed to identify their relationships. With mathematical modeling, diagrams of interactions between genes and proteins take on analytical power, and can reveal insights missed by verbal reasoning. Use the power of computers for all kinds of biological research, not just for circadian biology—or at least ask people like me for help! And although we know a lot of genes in some networks, we do not understand how they work as a system. For example, how do circadian clocks keep 24 h rhythms across a range of temperatures when individual biochemical reactions are temperature-dependent?

B: Okay, last question. The *Arabidopsis* clock loop had one loop yesterday, and two today. Modelers constructed simulations of the *Drosophila* and mammalian clocks that were rhythmic with just one loop, and then added a second loop when new components were identified (Leloup *et al*, 1999; Leloup and Goldbeter, 2003). Do you think you could predict how many feedback loops there are in a circadian clock? Two, three, four?

M: Good question. Let me get back to you on that one...

References

- Alabadi D, Oyama T, Yanovsky MJ, Harmon FG, Mas P, Kay SA (2001) Reciprocal regulation between TOC1 and LHY/CCA1 within the *Arabidopsis* circadian clock. *Science* **293**: 880–883
- Bacon F (1620) THE NEW ORGANON
- Forger DB, Peskin CS (2003) A detailed predictive model of the mammalian circadian clock. *Proc Natl Acad Sci USA* **100**: 14806–14811
- Hardin PE (2004) Transcription regulation within the circadian clock: the E-box and beyond. *J Biol Rhythms* **19**: 348–360
- Harmer SL, Hogenesch JB, Straume M, Chang HS, Han B, Zhu T, Wang X, Kreps JA, Kay SA (2000) Orchestrated transcription of key pathways in *Arabidopsis* by the circadian clock. *Science* **290**: 2110–2113
- Lawrence P (2004) Theoretical embryology: a route to extinction? *Curr Biol* **14**: R7–R8
- Leloup JC, Goldbeter A (2003) Toward a detailed computational model for the mammalian circadian clock. *Proc Natl Acad Sci USA* **100**: 7051–7056
- Leloup JC, Gonze D, Goldbeter A (1999) Limit cycle models for circadian rhythms based on transcriptional regulation in *Drosophila* and *Neurospora*. *J Biol Rhythms* **14**: 433–448
- Locke JCW, Southern MM, Kozma-Bognar L, Hibberd V, Brown PE, Turner MS, Millar AJ (2005) Extension of a genetic network model by iterative experimentation and mathematical analysis. *Mol Systems Biol* 28 June 2005; doi:10.1038/msb4100018
- Mizoguchi T, Wheatley K, Hanzawa Y, Wright L, Mizoguchi M, Song HR, Carre IA, Coupland G (2002) LHY and CCA1 are partially redundant genes required to maintain circadian rhythms in *Arabidopsis*. *Dev Cell* **2**: 629–641
- Tyson JJ (2004) A precarious balance. *Curr Biol* **14**: R262–R263

Extension of a genetic network model by iterative experimentation and mathematical analysis

Extended Synopsis

This study involves an iterative approach of mathematical modelling and experiment to develop an accurate mathematical model of the circadian clock in the higher plant *Arabidopsis thaliana*. Our approach is central to systems biology and should lead to a greater, quantitative understanding of the circadian clock, as well as being more widely relevant to research into genetic networks.

The day-night cycle caused by the Earth's rotation affects most organisms, and has resulted in the evolution of the circadian clock. The circadian clock controls 24-hour rhythms in processes from metabolism to behaviour; in higher eukaryotes, the circadian clock controls the rhythmic expression of 5-10% of genes. In plants, the clock controls leaf and petal movements, the opening and closing of stomatal pores, the discharge of floral fragrances and many metabolic activities, especially those associated with photosynthesis.

The relatively small number of components involved in the central circadian network makes it an ideal candidate for mathematical modelling of complex biological regulation. Genetic studies in a variety of model organisms have shown that the circadian rhythm is generated by a central network of between 6-12 genes. These genes form feedback loops generating a rhythm in mRNA production. One negative feedback loop in which a gene encodes a protein that, after several hours, turns off transcription is, in principle, capable of creating a circadian rhythm. However, real circadian clocks have proven to be more complicated than this, with interlocked feedback loops. Networks of this complexity are more easily understood through mathematical modelling.

The clock mechanism in the model plant, *Arabidopsis thaliana*, was first proposed to comprise a feedback loop in which two partially redundant genes, *LATE ELONGATED HYPOCOTYL (LHY)* and *CIRCADIAN CLOCK ASSOCIATED 1 (CCA1)*, repress the expression of their activator, *TIMING OF CAB EXPRESSION 1 (TOC1)*. We previously modelled this preliminary network and showed that it was not capable of recreating several important pieces of experimental data (Locke et al. 2005). Here, we extend the LHY/CCA1-TOC1 network in new mathematical models. To check the effects of each addition to the network, the outputs of the extended models are compared to published data and to new experiments.

As is the case for most biological networks, the parameter values in our model, such as the

translation rate of TOC1 protein, are unknown. We employ here an optimisation method which works well with noisy and varied data and allows a global search of parameter space. This should ensure that the limitations we find in our networks are due to the network structure, and not to our parameter choices.

Our final interlocked feedback loop model requires two hypothetical components, genes *X* and *Y* (figure 4), but is the first *Arabidopsis* clock model to exhibit such a good correspondence with experimental data. The model simulates a residual short-period oscillation in the *cca1;lhy* mutant, as characterised by our experiments. No single loop model is able to do this. Our model also matches experimental data under constant light conditions and correctly senses photoperiod. The model predicts an interlocked feedback loop structure similar to that seen in the circadian clock mechanisms of other organisms.

The interlocked feedback loop model predicts a distinctive pattern of *Y* mRNA accumulation in the wild type (WT) and in the *cca1;lhy* double mutant, with *Y* mRNA levels increasing transiently at dawn. We designed an experiment to identify *Y* based on this prediction. *GIGANTEA (GI)* mRNA levels fit very well to our predicted profile for *Y* (figure 6), identifying *GI* as a strong candidate for *Y*.

The approach described here could act as a template for experimental biologists seeking to extend models of small genetic networks. Our results illustrate the usefulness of mathematical modelling in guiding experiments, even if the models are based on limited data. Our method provides a way of identifying suitable candidate networks and quantifying how these networks better describe a wide variety of experimental measurements. The characteristics of new putative genes are thereby obtained, facilitating the experimental search for new components. To facilitate future experimental design, we provide user-friendly software that is specifically designed for numerical simulation of circadian experiments using models for several species (Brown 2004b).

Locke *et al.*, Mol. Sys. Biol. 2005, 28 June.

Extension of a genetic network model by iterative experimentation and mathematical analysis

James CW Locke^{1,2,3}, Megan M Southern¹, László Kozma-Bognár^{1,4}, Victoria Hibberd¹, Paul E Brown^{1,3,4}, Matthew S Turner^{2,3} and Andrew J Millar^{1,3,4,*}

¹ Department of Biological Sciences, University of Warwick, Coventry, UK, ² Department of Physics, University of Warwick, Coventry, UK and

³ Interdisciplinary Programme for Cellular Regulation, University of Warwick, Coventry, UK

* Corresponding author. Institute of Molecular Plant Sciences, University of Edinburgh, Rutherford Building, Mayfield Road, Edinburgh EH9 3JH, UK.

Tel.: +44 1316513325; Fax: +44 1316505392; E-mail: andrew.millar@ed.ac.uk

⁴ Present address: Institute of Molecular Plant Sciences, University of Edinburgh, Rutherford Building, Mayfield Road, Edinburgh EH9 3JH, UK

Received 5.4.05; accepted 7.6.05

Circadian clocks involve feedback loops that generate rhythmic expression of key genes. Molecular genetic studies in the higher plant *Arabidopsis thaliana* have revealed a complex clock network. The first part of the network to be identified, a transcriptional feedback loop comprising *TIMING OF CAB EXPRESSION 1 (TOC1)*, *LATE ELONGATED HYPOCOTYL (LHY)* and *CIRCADIAN CLOCK ASSOCIATED 1 (CCA1)*, fails to account for significant experimental data. We develop an extended model that is based upon a wider range of data and accurately predicts additional experimental results. The model comprises interlocking feedback loops comparable to those identified experimentally in other circadian systems. We propose that each loop receives input signals from light, and that each loop includes a hypothetical component that had not been explicitly identified. Analysis of the model predicted the properties of these components, including an acute light induction at dawn that is rapidly repressed by *LHY* and *CCA1*. We found this unexpected regulation in RNA levels of the evening-expressed gene *GIGANTEA (GI)*, supporting our proposed network and making *GI* a strong candidate for this component.

Molecular Systems Biology 28 June 2005; doi:10.1038/msb4100018

Subject Categories: metabolic & regulatory networks; plant biology

Keywords: biological rhythms; gene network; mathematical modelling; parameter estimation

Introduction

A circadian system that generates biological rhythms with a period of approximately 24 h is found in organisms ranging from cyanobacteria to mammals. The system is capable of sustained oscillations under constant environmental conditions and maintains synchrony with the environment by entraining to rhythmic cues of the day/night cycle, especially input signals from light. Circadian rhythms allow diverse biological processes to occur at times in the day/night cycle (phases) that confer a selective advantage: it might be important, for example, that a particular process occurs in anticipation of a light/dark transition. The molecular mechanism of the circadian clock has been studied in several model organisms. A shared feature of these systems appears to be that the rhythms are generated by the interactions of rhythmically expressed genes that form positive and negative feedback loops (Dunlap, 1999).

Computational models of these feedback loops have been developed for a variety of organisms including the fungus *Neurospora crassa* (Leloup *et al.*, 1999; Ruoff *et al.*, 2000, 2001), the fruitfly *Drosophila melanogaster* (Tyson *et al.*, 1999; Ueda *et al.*, 2001; Smolen *et al.*, 2004) and the mouse (Forger and Peskin, 2003; Leloup and Goldbeter, 2003). These models have

shown that, within defined parameter ranges, the regulatory networks proposed from experimental data are capable of reproducing the main characteristics of circadian rhythms. Simple models indicate that a single feedback loop is sufficient to generate robust 24 h oscillations (Leloup *et al.*, 1999; Ruoff *et al.*, 2000, 2001), although the experimental data show that a series of interlocked feedback loops are important for generating the observed circadian rhythms (Glossop *et al.*, 1999; Lee *et al.*, 2000). It is an open question why circadian systems have evolved a more complex structure. Recent mathematical studies proposed that interlocked feedback loops increase the flexibility of regulation during evolution (Rand *et al.*, 2004) and enhance precision (Stelling *et al.*, 2004).

In higher plants, the circadian system controls many processes, including leaf movement, photoperiodism, and photosynthesis. The first part of the clock mechanism in *Arabidopsis* to be identified was proposed to comprise a feedback loop, in which two partially redundant genes encoding similar DNA-binding proteins, *LATE ELONGATED HYPOCOTYL (LHY)* and *CIRCADIAN CLOCK ASSOCIATED 1 (CCA1)*, repress the expression of their activator, *TIMING OF CAB EXPRESSION 1 (TOC1)* (Alabadi *et al.*, 2001). We refer to this single loop as the *LHY/CCA1-TOC1* network. Light can activate *LHY* and *CCA1* expression, possibly by several

mechanisms (Wang and Tobin, 1998; Martinez-Garcia *et al*, 2000; Kim *et al*, 2003), providing a potential pathway for light input to the clock. Several other rhythmically expressed genes have been associated with the *Arabidopsis* circadian system (reviewed in Eriksson and Millar, 2003). For example, *EARLY FLOWERING 3 (ELF3)* (McWatters *et al*, 2000; Covington *et al*, 2001), *GIGANTEA (GI)* (Fowler *et al*, 1999; Park *et al*, 1999) and *EARLY FLOWERING 4 (ELF4)* (Doyle *et al*, 2002) are genes expressed in the evening. Mutations in these genes strongly affect circadian rhythms and reduce *LHY* and *CCA1* gene expression, but their functions have not been located in more detail within the *LHY/CCA1-TOC1* network.

The *LHY/CCA1-TOC1* network alone did not readily account for some aspects of circadian behaviour, such as the long delay between *TOC1* transcription in the evening and *LHY/CCA1* activation the following morning (Alabadi *et al*, 2001; Salome and McClung, 2004). Our previous differential equation model of the *LHY/CCA1-TOC1* loop confirmed that this network failed to fit certain experimental data and quantitatively tested a range of its predicted behaviours (Locke *et al*, 2005). For example, we showed that the *LHY/CCA1-TOC1* loop could not reproduce the short-period phenotype of plants that carry loss-of-function mutations in either *LHY* or *CCA1* (Green and Tobin, 1999; Mizoguchi *et al*, 2002; Locke *et al*, 2005). The delay required for the model to fit appropriate phases of gene expression was estimated at 12 h between *TOC1* transcription and *LHY/CCA1* activation (Locke *et al*, 2005). There is no obvious mechanism for this delay, reinforcing the suggestion that *TOC1* protein may activate *LHY* and *CCA1* expression indirectly.

Here, we extend the *LHY/CCA1-TOC1* network beyond the structures inferred solely from data, in new mathematical models that we use to direct further experimentation. To check the effects of each addition to the network, the outputs of the extended models are compared to published data and to the new experiments. The biochemical parameter values required in the model are constrained by the time-series data but have not been measured directly, so we made a global search of parameter space, in contrast to previous clock models. This reduces the possibility that problems with the model are due to a particular set of parameter values, allowing us to focus on the network structure. The fit of the model to experimental data is dramatically improved by the addition of two hypothetical components, *X* and *Y*, to the model. Their properties are predicted; *X* remains to be identified, whereas experimental analysis shows that *GI* has several of the properties predicted for *Y*. The model suggests further experiments: we expect that iterative application of modelling and experiment will facilitate a more quantitative understanding of the *Arabidopsis* circadian clock.

Results

Limitations of the *LHY/CCA1-TOC1* network

Our previous simulations using the single-loop *LHY/CCA1-TOC1* network (Supplementary Figure 1) showed that it was possible for this network to correctly reproduce the phases of *TOC1* and *LHY* RNA accumulation in wild type (WT) under light-dark cycle (LD) 12:12. (In this and subsequent models,

we use a single gene, *LHY*, to represent both *CCA1* and *LHY* functions; see Supplementary text.) However, simulated *TOC1* RNA levels remained high until *LHY* protein accumulated, rather than falling after dusk as observed (Mizoguchi *et al*, 2002). This was exaggerated by halving the *LHY* mRNA translation rate in the simulation (representing *lhy* or *cca1* loss-of-function mutants), which incorrectly predicted a long-period phenotype. Thus, there must be another factor responsible for reducing *TOC1* expression, which is not modelled by this network (Locke *et al*, 2005).

Studies of a fluorescent protein, *TOC1* fusion protein, suggest an additional limitation (Mas *et al*, 2003b). The *TOC1* fusion was shown to be close to its minimum abundance before dawn under LD12:12, whereas according to the single-loop *LHY/CCA1-TOC1* network, *TOC1* should be activating *LHY* transcription maximally at that time (Locke *et al*, 2005). This suggests that either the active form of *TOC1* is present at a far lower concentration than bulk *TOC1* protein, perhaps in a complex, or that an additional, *TOC1*-dependent component is the direct activator of *LHY* and *CCA1*.

A third problem is that the *LHY/CCA1-TOC1* network did not respond to day length (simulated gene expression profiles were identical in LD cycles with long and short photoperiods, data not shown), whereas it is clear experimentally that the clock has a later phase under longer photoperiods (Millar and Kay, 1996; Roden *et al*, 2002). This limitation occurs because light input to this network is modelled only by the activation of *LHY* expression at dawn, so the model is insensitive to light at the end of the photoperiod. Indeed, *LHY* and *CCA1* expression fall to a low level before the end of a 12 h photoperiod (Kim *et al*, 2003), so another mechanism is required to mediate light input at the end of the day.

Model one—the *LHY/CCA1-TOC1-X* network

We extended the single-loop *LHY/CCA1-TOC1* network by adding components that would address these limitations, as directed by the experimental data. After each addition, we tested network parameters until it became clear that the new network could not account for further experimental data. We identified optimal parameters for the most promising of the extended, single-loop models, which we term the *LHY/CCA1-TOC1-X* network (Figure 1). Firstly, light activation of *TOC1* transcription was included to provide light input at the end of the day and, conversely, to reduce *TOC1* activation immediately after lights-off. Secondly, an additional gene *X* was added to the network after *TOC1*, with nuclear *X* protein as the immediate activator of *LHY* instead of nuclear *TOC1*. Thirdly, as the F-box protein ZEITLUPE (*ZTL*) has been shown to degrade *TOC1* protein more effectively during the night (Mas *et al*, 2003b), we added this factor into our network equations (see Supplementary text).

Figure 1 shows the simulated expression profiles for the *LHY/CCA1-TOC1-X* network using the optimal parameter set (Supplementary Table 1). *TOC1* RNA levels peak at dusk in WT under LD12:12, and *LHY* RNA levels at dawn. The model allows *TOC1* mRNA levels to drop before *LHY* levels rise, as observed in experiment. Including gene *X* within the model permits simulated *TOC1* protein levels to fit well with the published data (Supplementary Figure 2). *ztl* mutants were

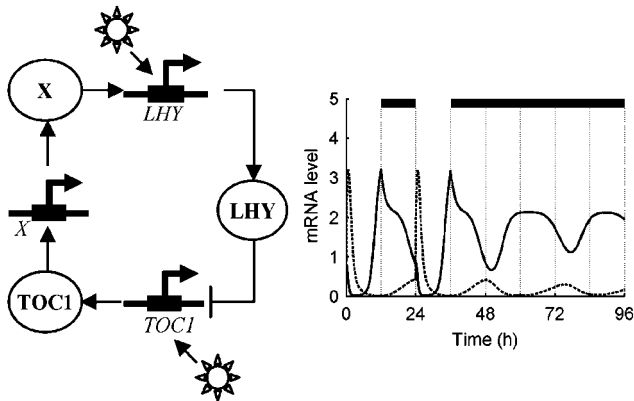


Figure 1 The single-loop *LHY/CCA1*–*TOC1*–*X* network. Left panel: Network diagram. *LHY* and *CCA1* are modelled as a single gene, *LHY* (genes are boxed). Nuclear and cytoplasmic protein levels are grouped for clarity (shown encircled) and degradation is not shown. Light acutely activates *LHY* transcription at dawn and activates *TOC1* transcription throughout the day. *TOC1* activates a putative gene *X*, which in turn activates *LHY*. Nuclear *LHY* protein represses *TOC1* transcription. Right panel: Simulation of mRNA levels for the optimal parameter set. In all figures, filled box above the panel represent dark interval and open or no box represent light interval. *LHY* mRNA (dotted line) peaks at dawn in LD12:12 and *TOC1* (solid line) falls after dusk, due to the loss of light activation.

modelled by reducing the degradation rates of *TOC1* protein in the cytoplasm and the nucleus by 50%. This results in a long-period phenotype, with a period of 32 h, similar to or longer than the period of *ztl* mutants (Mas et al, 2003b). A prediction of *X* mRNA and protein levels is also possible (Supplementary Figure 2): *X* mRNA peaks in the middle of the night under LD12:12 and nuclear *X* protein levels peak at dawn. Strong *x* mutants have the same predicted phenotype as the strongest phenotype of *toc1* loss-of-function mutants, causing arrhythmia due to the lack of *LHY* activation (data not shown). The pattern of *X* mRNA accumulation and its mutant phenotype are similar to those of characterised genes such as *ELF4* (Doyle et al, 2002). However, this model still incorrectly predicts a long period in the simulated *cca1* single mutant (Supplementary Table 2) and the strong, LL activation of *TOC1* transcription causes several problems, for example the model becomes arrhythmic under LD cycles with long photoperiods (data not shown).

Experimental characterisation of the *cca1;lhy* double mutant

The response of circadian phase to day length (Millar and Kay, 1996; Roden et al, 2002) strongly suggested that the circadian system receives at least one light input in addition to the activation of *LHY* and *CCA1* expression, yet simulations with the *LHY/CCA1*–*TOC1*–*X* network indicated that this was unlikely to be a simple light activation of *TOC1* transcription. We sought more direct evidence for this light input by characterising circadian rhythms in the *cca1;lhy* double loss-of-function mutant. RNA data for *cca1;lhy* mutants in constant conditions show a damping, short-period oscillation (Alabadi et al, 2002; Mizoguchi et al, 2002), which has been described as arrhythmia. We repeated these experiments using luciferase

imaging (Figure 2). In the *cca1;lhy* mutant, promoter activity of *CCA1* and of the clock output genes *CCR2* and *CAB2* showed an 18 h rhythm for at least three cycles in constant light (LL), which subsequently lost amplitude. The rhythm is more robust in LL but is also apparent in constant dark (DD) (Figure 2). The double mutant retains a regulatory network capable of supporting rhythmic gene expression.

Reproducible entrainment of the double mutant by LD cycles was implicit in previous reports, suggesting that entrainment by light is still possible in the residual network (Alabadi et al, 2002; Mizoguchi et al, 2002) (Figure 2). To test this more stringently, we generated a phase transition curve (PTC) for the WT and double mutant (Figure 3). The PTC

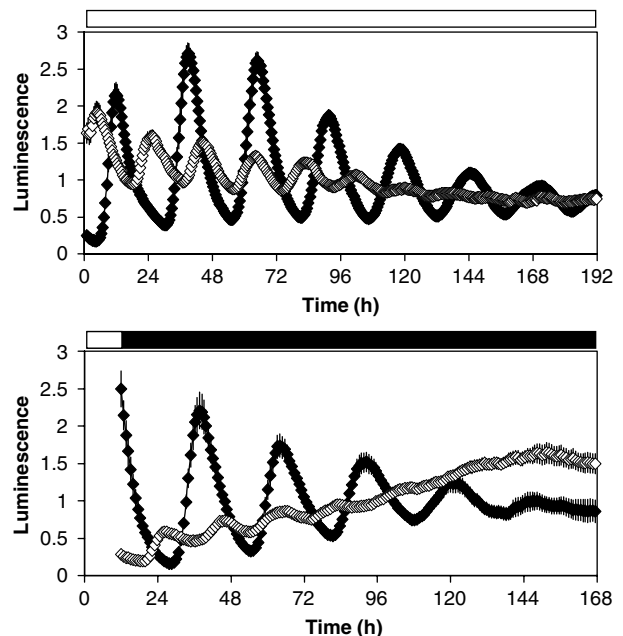


Figure 2 Expression of *CCR2:LUC+* in WT (filled diamonds) and *cca1-11;lhy-21* double mutant (open diamonds) plants in LL (top) and DD (bottom). Luminescence of each seedling was normalised to its mean value over the entire time course. Data are averages of normalised luminescence from WT seedlings in LL $n=16$, in DD $n=18$, *cca1;lhy* seedlings in LL $n=13$, in DD $n=15$. Error bars represent one s.e.m., often within symbols.

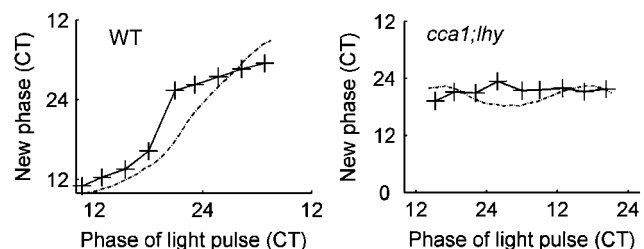


Figure 3 PTC for WT (left panel) and *cca1;lhy* double mutant (right panel). Red light pulses ($15 \mu\text{mol m}^{-2} \text{s}^{-1}$ for 1 h) were administered at 3 h intervals to *CCR2:LUC+* plants in DD. The new phase of the rhythm induced by the light pulses was converted to circadian time (CT, 24ths of the free-running period) and plotted against the circadian time of light treatment (solid lines). Simulated phase responses are represented by dashed lines, and show simulated response of the interlocked feedback loop model to a 1 h light pulse. Phase marker for simulation was *TOC1* mRNA peak, compared to *CCR2:LUC+* peak in data.

shows the response of an oscillator to a resetting stimulus and is plotted as the phase to which the oscillator is set ('new phase'), for each phase at which the resetting stimulus is applied ('old phase'). In WT, light pulses induced phase delays during the early subjective night and phase advances during the late subjective night, whereas relatively small phase shifts were elicited during the subjective day. The WT showed a type 1 (weak) resetting pattern with less than 6 h maximal phase shifts, in contrast to the type 0 (strong) resetting observed in a previous report (Covington *et al*, 2001), probably due to the lower fluence of our light stimulus. In contrast, the double mutant showed type 0 resetting: irrespective of the phase of the light stimulus, the clock was reset to a narrow phase range (circadian time (CT) 20–23). Light input to a residual, rhythmic network remained without *LHY* and *CCA1* function, leading us to add a second, light-responsive feedback loop to produce our final model.

Model two—the interlocked feedback loop network

Removing *LHY* function from the single-loop models prevents any oscillation (data not shown), so none of these models can reproduce the entrainable, damped rhythms observed in *cca1;lhy* plants. We therefore developed an interlocked feedback loop network that is capable of oscillation in simulated *cca1;lhy* double mutants (Figure 4). A hypothetical gene *Y* activates *TOC1* transcription and *TOC1* protein represses *Y* transcription, forming a feedback loop. The proposal that *TOC1* has a negative function as well as a positive one is novel. Light input into this loop occurs via transcriptional activation of *Y* rather than of *TOC1*; there is as yet no evidence of direct

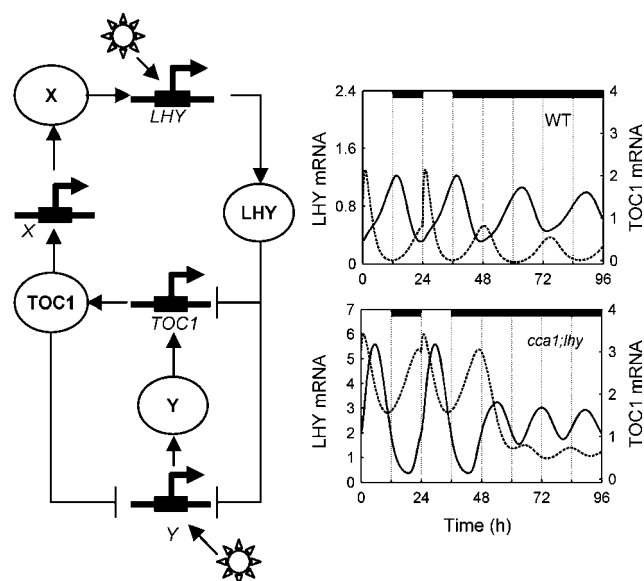


Figure 4 The interlocked feedback loop network. Left panel: Network diagram. Compared to Figure 1, *TOC1* is activated by light indirectly via hypothetical gene *Y*. *Y* activates *TOC1* transcription and both *LHY* and *TOC1* repress *Y* transcription, forming a second feedback loop. Right panel: Simulation of *LHY* (dashed line) and *TOC1* (solid line) mRNA levels for the optimal parameter set, representing WT (top) and *cca1;lhy* double mutant (bottom) in DD. Translation rate of *LHY* mRNA in simulated mutant is 1/1000 WT value. Period of WT in DD is 26 h and period of mutant is 17 h.

light activation of *TOC1* (Makino *et al*, 2001). Light input to *Y* can both be through an acute response at dawn similar to that for *LHY* and as a constant activation term throughout the day. *Y* is also repressed by *LHY*, as this allowed the network to fit the WT as well as the *cca1;lhy* experimental data. *LHY* therefore acts as a powerful delaying factor in the early day, when it inhibits expression of both *TOC1* and *Y*.

Optimal parameters for the interlocked feedback loop network (Supplementary Table 3) were identified (see Computational methods). The optimised model achieved a good fit to experimental results that were specifically required by the optimisation process, showing that the proposed network is sufficient to explain these data. Simulations of the WT and *cca1;lhy* mutant using the optimal model fit well to RNA expression profiles in DD and LD12:12 (Figures 5A and B). For the WT simulation (Figure 4), *LHY* mRNA peaks at dawn, *TOC1* at dusk, and the oscillations follow a stable limit cycle with a period of 26 h in DD. *TOC1* mRNA levels under LD cycles are shown to increase at dawn. This is due to the induction of *Y* by light activating *TOC1* expression, overcoming the repression by *LHY* protein. The simulation of *cca1;lhy* gives a low-amplitude oscillation in DD with a 17 h period (Figure 4), as observed experimentally (Figure 2). Under LD12:12, *TOC1* mRNA oscillates with an early peak phase in the double mutant, ~5 h after dawn, as specified in the optimisation. The rhythm of *TOC1* expression in the double

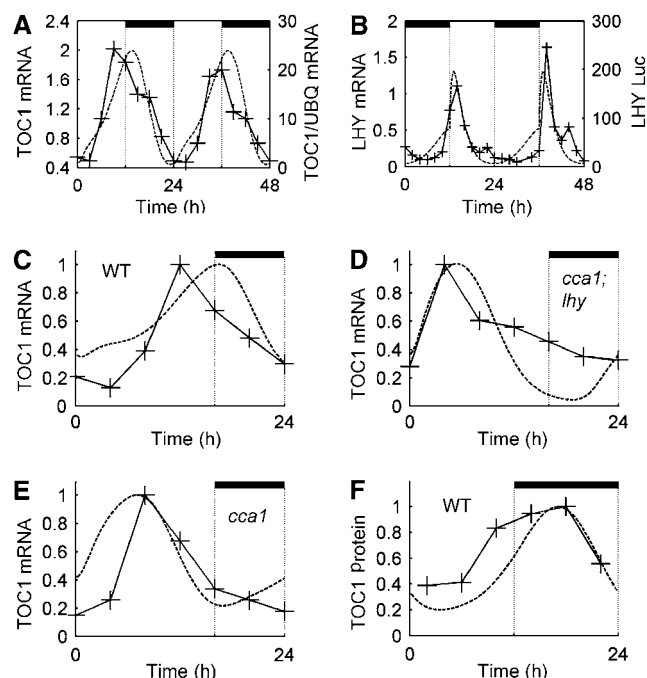


Figure 5 Comparison of interlocked feedback loop simulations (dashed line) under LD to data (solid line). (A) *TOC1* mRNA levels in WT plants entrained to LD12:12, left axis; *TOC1* mRNA levels relative to UBIQUITIN (UBQ) (Makino *et al*, 2000), right axis. (B) *LHY* mRNA levels in WT plants entrained to LD12:12, left axis; data from Kim *et al* (2003), right axis. (C–E) *TOC1* mRNA levels in WT (C), *cca1;lhy* mutant (D) and *cca1* mutant (E) entrained to LD16:8; data from Mizoguchi *et al* (2002). Translation rate of *LHY* in simulated *cca1* is set to 1/2 WT value. Highest value of data and simulation is set to 1, for each panel. (F) *TOC1* protein levels for WT simulation entrained to LD12:12; *TOC1* fusion protein data from Mas *et al* (2003b).

mutant also shows a higher amplitude than WT (Figure 4), which is observed experimentally (Mizoguchi *et al*, 2002) but was not specified during optimisation. Figures 5C and D show similar expression profiles for simulated and observed (Mizoguchi *et al*, 2002) *TOC1* mRNA in the WT and *cca1;lhy* mutant under LD16:8 (note that normalisation of data and simulated values obscures the change in amplitude in this figure). *TOC1* mRNA anticipates dawn in the simulation of the *cca1;lhy* double mutant, which has not been so clearly observed in published experimental data and points to an area for future experimentation.

Analysis and validation of the interlocked feedback loop network

The interlocked feedback loop model with the optimal parameters not only fits the above data but its behaviour is also robust to parameter changes. This is widely thought to be a realistic requirement for models of biological regulation, because effective parameter values may be poorly buffered in biology. Changes in the period and amplitude of *TOC1* RNA oscillation under LL were examined after a 5% increase or decrease of each parameter value in turn (Supplementary Figure 3). The resulting change in period varied from 0 to 4%. As for previous clock models (Smolen *et al*, 2004; Locke *et al*, 2005), some parameters are more sensitive to change than others. The most sensitive parameters are those involved in *TOC1* degradation, X translation and X nuclear transport. The period and amplitude of this model are much less sensitive to parameter changes than the single-loop *LHY/CCA1-TOC1* model (data not shown), suggesting that some of the weaknesses of the single-loop model have been overcome.

Simulations using the optimal parameter set also fit well to several experimental results that were not specified in the optimisation, giving additional support for the proposed network structure. This is the first model that fits well to LL data for *LHY* and *TOC1* mRNA levels. The WT period in LL is correctly shorter (25 h) than the period in DD (26 h; Supplementary Figure 4) although this effect is less than that observed experimentally. The rhythms in LL generally have a higher amplitude than in DD, as observed. The model correctly predicts the short-period phenotype of *cca1* and *lhy* single mutants in LL and DD (Supplementary Table 2), and the early phase of *TOC1* RNA expression in the single mutant under LD12:12 (Figure 5E). The single mutants were simulated by halving the *LHY* mRNA translation rate. Simulated overexpression of *LHY* produced arrhythmia with low levels of *TOC1* mRNA (data not shown), as observed in plants that overexpress *LHY* or *CCA1* (Schaffer *et al*, 1998; Wang and Tobin, 1998; Alabadi *et al*, 2001). Protein levels are also well fitted: simulated LHY protein levels (data not shown) peak 1–2 h after *LHY* mRNA levels, as observed (Kim *et al*, 2003). Figure 5F compares simulated and measured (Mas *et al*, 2003b) *TOC1* protein levels in WT, showing low levels at dawn in both cases. The optimal parameter set has minimised the light regulation of *TOC1* degradation (<1% of total *TOC1* degradation), indicating that light-regulated degradation (Mas *et al*, 2003b) is not required to fit these data. Simulation of *ztl* mutants by halving the total *TOC1* degradation rate results in a

28 h period phenotype, again similar to that observed in *ztl* mutants (Mas *et al*, 2003b). A simulated *toc1* mutant results in lower levels of *LHY* mRNA as expected from experiment (Alabadi *et al*, 2001), and simulated *TOC1* overexpression is predicted to increase *LHY* mRNA levels. The observed decrease in *LHY* mRNA where *TOC1* is overexpressed (Makino *et al*, 2002; Mas *et al*, 2003a; Somers *et al*, 2004) remains paradoxical, since one would expect overexpressing an activator of *LHY* to cause its levels to rise.

Simulations of the WT and *cca1;lhy* double mutant PTCs were performed, as shown in Figure 3. Both simulations are similar to our experimental data, with a type 1 PTC in the WT and a type 0 PTC in the double mutant. Increasing the light level in the WT simulation results in a type 0 PTC (data not shown), as previously observed (Covington *et al*, 2001). As expected, the entrained phase of the interlocked feedback model is photoperiod responsive (Supplementary Figure 5), with simulated mRNA levels peaking later under longer photoperiods, as observed (Roden *et al*, 2002; Yanovsky and Kay, 2002). Light input to *Y* allows the network to respond to light throughout the day. This network will therefore be a good starting point for models of the photoperiod sensor involved in flowering time. The photoperiod range of entrainment is approximately from 3:16 h light for a 24 h period, and the simulations remain entrained for an approximate period range of 22–30 h, where half the period is in light and half in dark. At the end of the ranges, entrainment produces a beat in the amplitude, although with little effect on phase. The balance of light input to *LHY*, *Y* and *ZTL* should now be examined in greater detail to determine how their contributions affect circadian entrainment.

GIGANTEA is a candidate for *Y*

The interlocked feedback model predicts a distinctive pattern of *Y* mRNA accumulation in the WT and double mutant (Figure 6). *Y* mRNA levels peak at the end of the day, but also increase transiently at dawn due to the acute light response of *Y* transcription. This early expression is quickly repressed by rising *LHY* protein levels, delaying the peak in *Y* mRNA level until after *LHY* protein is degraded at the end of the day. *Y* transcription is then repressed as *TOC1* protein levels begin to rise during the night (Figure 4). In the *cca1;lhy* double mutant, however, the light activation of *Y* at dawn is de-repressed, resulting in a much stronger activation than in WT, and causing *Y* mRNA levels to peak soon after dawn. No gene with this expression pattern had been observed experimentally.

In order to identify *Y*, we analysed the transcript abundance of clock-affecting genes with peak RNA levels in the evening in WT and *cca1;lhy* double mutant seedlings. Tissue samples were harvested across the light–dark transitions in one LD cycle, followed by one cycle in LL. *GI* mRNA levels fitted very well to our predicted mRNA profiles for *Y* (Figure 6). *GI* was shown to be significantly but transiently light activated in the WT and had a very strong light response in the double mutant. The subsequent circadian peak also fitted closely to the prediction for *Y* mRNA, including the 12 h phase advance in the mutant relative to WT (Figure 6). The tentative identification of *Y* as *GI* allowed us to test whether *Y* in our model fitted additional, published results for *GI*; indeed, further data do

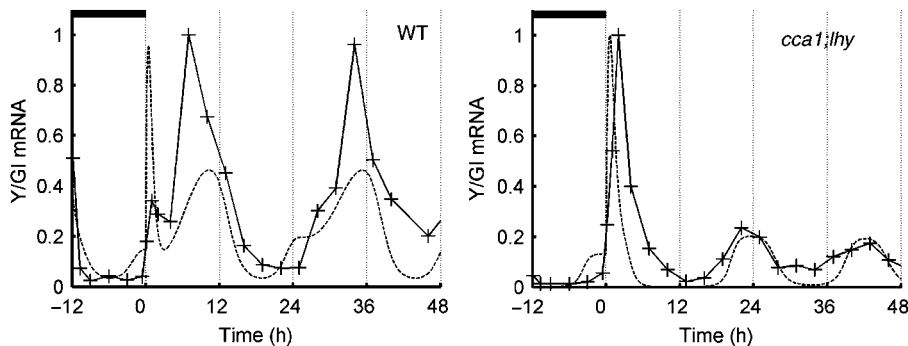


Figure 6 *GI* is a candidate gene for *Y*. Simulated *Y* mRNA levels under LD12:12 and LL (dashed line). Data for *GI* mRNA levels (crosses), assayed by quantitative RT-PCR relative to the *ACT2* control, from samples harvested at the times indicated. Left panel, WT; right panel, *cca1;lhy*. Highest value of data and simulation is set to 1, for each panel.

support this proposed function of *GI*. *GI* mRNA is at a low, arrhythmic level in plants that overexpress *LHY* (Fowler *et al*, 1999) or *TOC1* (Makino *et al*, 2002): this agrees with model predictions (data not shown) and occurs because both *LHY* and *TOC1* repress *Y* transcription (Figure 4). The sequence of the *GI* promoter includes several Evening Elements, the putative binding sites for *LHY* (Harmer *et al*, 2000). *gi* loss-of-function mutations result in low-amplitude circadian rhythms, with low levels of *LHY* and *CCA1* RNA and either shorter or longer circadian periods (Fowler *et al*, 1999; Park *et al*, 1999) or, in some conditions, in arrhythmia (A Hall, personal communication). A simulated null mutation of *Y* indeed results in still lower *LHY* transcription and therefore in arrhythmia. If another gene in *Arabidopsis* can substitute for a fraction of *Y* function, then null mutants will avoid arrhythmia. Supplementary Figure 6 shows the oscillation of *LHY* mRNA levels in a simulated partial loss-of-function *y* mutant, where *Y* translation rate has been halved compared to the WT rate. As observed in *gi* mutants, the oscillations have reduced *LHY* expression and a low amplitude both in LD cycles and in LL (Mizoguchi *et al*, 2002).

Discussion

We use a joint, experimental and mathematical approach to understand the plant circadian clock as an example of a regulatory subnetwork that is not completely identified. We start from the first proposed feedback loop of the circadian clock mechanism in *Arabidopsis*, the *LHY/CCA1-TOC1* network (Alabadi *et al*, 2001). Comparing model predictions with experimental results, we have progressively incorporated additional components and interactions identified by molecular genetics or inferred from physiological analysis. The final, interlocking loop model accounts for a greater range of data than the single-loop models, including the entrainable, short-period oscillations in the *cca1;lhy* double mutant. In developing this model, we included two putative genes *X* and *Y*, and used experiments designed from the model predictions to identify *GI* as a candidate gene for *Y*. Additional components of the plant circadian clock mechanism almost certainly remain to be identified, but we believe that this model is a

significant step forward in understanding of the timing mechanism.

The prediction of new components is a particularly beneficial outcome from formal modelling of a system that has not been completely identified by experiment. Mathematical models, in contrast to intuitive reasoning, can produce quantitative predictions of dynamic processes that allow detailed experimental design. This was important: the acute light activation of *Y* in WT was predicted to be very transient (peak 25 min after lights-on; Figure 6), allowing us to target our tissue sampling to the appropriate interval, whereas conventional sampling had obscured this induction of *GI* RNA (Mizoguchi *et al*, 2002). The interlocked feedback model now highlights the importance of *GI* as a component of light input to the clock, a role that had not previously been emphasised and should now be tested in greater detail. The activation of *TOC1* by *GI* in an interlocked feedback loop is also a new proposal, which is consistent with the timing of peak *GI* expression before *TOC1*. Mutants that remove both the loops, such as the *lhy;cca1;gi* triple mutant, should now be tested to determine whether further oscillating subnetworks remain in their absence. A recent study has suggested the existence of a feedback loop between *APRR9/APRR7* and *LHY/CCA1* (Farre *et al*, 2005). Including this loop would not affect our conclusions on the residual network in the *cca1;lhy* double mutant, which would lack this additional loop. As more data become available, it will be possible to determine how the *PRR* genes should be included into the network model. The component(s) that activate *CCA1* and *LHY* at the end of the night remain to be identified: the model predicts the likely accumulation pattern of such a component, *X*. The level of detail in such predictions is obviously limited by the data upon which the model is based, so including statistical measures of uncertainty with the predictions will be increasingly important (Brown and Sethna, 2003).

Each model makes further, qualitative predictions that appear robust and readily testable. The constant activation of *TOC1* by light reproducibly caused arrhythmia of the *LHY/CCA1-TOC1-X* model under long photoperiods or LL, for example, which is not observed in WT plants. This highlights the importance of rhythmic inhibition of the light input (Roenneberg and Merrow, 2002), which is a wide spread feature of clocks (Fleissner and Fleissner, 1992; Jewett *et al*,

1999). It is reminiscent of the *ELF3*-dependent zeitnehmer function observed in *Arabidopsis* (McWatters *et al*, 2000; Covington *et al*, 2001). In the interlocked loop model, repression of *Y* by *LHY* and by *TOC1* are sufficient to gate the light activation of *Y*, so we had no justification for further additions to this model. Clearly, such models should be interpreted with caution, because undiscovered components cannot be included explicitly. A model that accurately recapitulates the regulation of known components is very likely to have captured the relevant effects of the 'hidden' components. The model can advance understanding and make useful predictions but might not capture the real number or mechanism of the hidden components. For example, we model the direct activator of *LHY* and *CCA1* as the product of a *TOC1*-activated gene, *X*, which could be a minor population of modified *TOC1* protein or *TOC1*-dependent protein complex. We assume that *Y* mediates both the second light input and the additional feedback loop for parsimony, which is now supported by data on *GI*, although these functions could in principle be split among several components.

The importance of the light input pathways in our models was to be expected, because the plant circadian system is known to interact with multiple photoreceptor pathways in a complex fashion (reviewed in Fankhauser and Staiger, 2002; Millar, 2003). The tracking of multiple phases during entrainment is thought to require at least two light inputs to two feedback loops (Rand *et al*, 2004), for example, which are present in our final model. The entrainment patterns of the *Arabidopsis* clock under different photoperiods (Millar and Kay, 1996) indicate that the phase of the clock does not simply track dawn. Therefore, the clock must receive light input(s) at times other than the dark-light transition. In our model, *LHY* allows light input at dawn, while input to *Y* and *ZTL* is potentially effective throughout the day. The known input photoreceptors could in future be explicitly included, providing quantitative estimates of their function for comparison to data from plant photobiology. Similarly, the models will help to reveal how the circadian output pathways allow the few genes of the clock to control over a thousand rhythmically regulated genes in the *Arabidopsis* genome (Harmer *et al*, 2000). However, the complexity of such biological networks is likely to limit the quantitative accuracy of early models, so the potential value of simplified experimental model systems that facilitate the link to mathematical analysis is clear. These will include synthetic gene networks in microbial hosts but also 'reduced' systems: we have recently characterised circadian rhythms in seedlings without light exposure, in which both the complexity of the circadian system and the number of clock-controlled target genes are greatly reduced (A Hall *et al*, unpublished results).

Materials and methods

Plant materials and growth conditions

Wassilewskija (Ws) WT and *cca1-11;lhy-21* (termed *cca1;lhy*) double mutants in the Ws background (Hall *et al*, 2003) were used in all experiments. Luciferase reporter gene fusions containing the promoter region of *CCA1* (*CCA1:LUC+*), *CHLOROPHYLL A/B-BINDING PROTEIN2* (*LHCB1.1*) (*CAB2:LUC+*) and *COLD AND CIRCADIAN REGULATED 2* (*CCR2:LUC+*) were introduced into Ws and mutant

plants by *Agrobacterium*-mediated transformation, essentially as described (Hall *et al*, 2003). For each genotype and reporter, three independent transgenic lines were tested in each experiment; all gave very similar results. Light sources were as described (Hall *et al*, 2003). Seedlings for luminescence analysis were grown under 12 h light:12 h dark cycles (LD12:12), as described (Hall *et al*, 2003). Seedlings for RNA analysis were grown under LD12:12 comprising 13–20 $\mu\text{mol m}^{-2} \text{s}^{-1}$ red light for 6 days, followed by constant 13–20 $\mu\text{mol m}^{-2} \text{s}^{-1}$ red light for 3 days. Samples of ~150 μl packed volume of seedlings were harvested into *RNAlater* buffer (Ambion, Huntingdon, UK) to stabilise RNAs, starting in the last cycle of entrainment.

Luminescence and rhythm analysis

Luminescence of individual seedlings was measured with an automated luminometer (Doyle *et al*, 2002). Rhythmic data were analysed using the fast Fourier transform nonlinear least squares procedure (Plautz *et al*, 1997) through the Biological Rhythms Analysis Software System, available online (Brown, 2004a). Variance-weighted mean periods and standard errors are presented. To create PTCs, seedlings expressing the *CCR2:LUC+* reporter were grown and entrained as above, and then transferred to DD at the predicted time of lights-off. Luminescence signals were monitored for 5 days in DD. After 24 h in DD, separate populations of seedlings were treated with 15 $\mu\text{mol m}^{-2} \text{s}^{-1}$ red light for 1 h and returned to DD at 3 h intervals. The free running period and phase of the control (nontreated WT and mutant) plants was used to calculate the circadian time of the light treatments ('old phase'). The time of the next peak of *CCR2:LUC+* expression was determined in the treated plants and circadian time of the 'new phase' set at the light pulse was estimated using the cognate period value.

RNA analysis

Seedlings were homogenised in RLT buffer (Qiagen, Crawley, UK) using a MixerMill MM300 at a frequency of 30 s^{-1} for 3 min with a 5 mm stainless steel cone ball (Retsch, Leeds, UK). Total RNA was isolated using a Plant RNeasy kit and RNase-free DNase (Qiagen, Crawley, UK) according to the manufacturer's instructions. A 1 μg portion of total RNA was reverse-transcribed using the RevertAid cDNA kit (Fermentas, Helena Biosciences, Sunderland, UK) with random hexamer primers, according to the manufacturer's instructions. *GI* sequence abundance in each cDNA sample was assayed by quantitative PCR in an ABI PRISM 7700 using ABI SYBRgreen PCR Mix (Applied Biosystems, Warrington, UK) in a final volume of 15 μl . *GI* sequence abundance was normalised relative to *ACTIN2* (*ACT2*), using a cDNA dilution series for each primer set in each experiment. The following primers were used:

GI forward primer AATTCAGCACGCGCCTATTG,
GI reverse primer GTTGCTTCTGCTGCAGGAACCT;
ACT2 forward primer CAGTGTCTCGATCGGAGGAT,
ACT2 reverse primer TGAACAATCGATGCACCTGA, each at 300 nM.

Each RNA sample was assayed in triplicate. Data shown are a representative trace from two independent biological replicates that gave very similar results.

Computational methods

As there is too little data to discriminate *LHY* from *CCA1* regulation and function, we combine them in the single model component '*LHY/CCA1*' in order to simplify our models (see Supplementary text); for brevity, we refer to this joint component as *LHY*, as in our previous work. Our method of parameter estimation uses a cost function, which is based on reproducible, qualitative features of experimental data, to score the performance of a model with a test parameter set. The cost function is minimised by the optimisation procedure described (Locke *et al*, 2005). A low cost (indicating a good fit) is obtained for parameter sets that allow the model of WT plants to be entrained in LD12:12

cycles, with *LHY* RNA levels that peak at dawn, *TOC1* RNA levels that peak at dusk and oscillations with a period greater than 24 h in DD. As there is only limited, noisy experimental data for the mRNA oscillation of *TOC1* and *LHY* in DD, it is difficult to verify that the *TOC1* and *LHY* mRNA levels converge to a stable limit cycle. The cost function only requires that *LHY* and *TOC1* mRNA levels oscillate with slow damping in DD, giving a reasonable score if the size of oscillation has dropped by 25% over 300 h (Strayer *et al*, 2000; Kim *et al*, 2003). Developing the model based on LD and DD data allowed subsequent testing of the model by comparison to the larger amount of experimental data available from LL conditions.

The interlocked feedback loop network proposed here was scored both as a model of WT and of the *cca1;lhy* mutant. The double mutant was simulated by reducing the translation rate of *LHY* to 1/1000th of its WT value. This simulated mutation led to arrhythmia in all the single-loop models (data not shown). Additional terms were introduced to the cost function to score models of the double mutant, specifying entrainment under LD12:12 with peak *TOC1* expression 5 h after dawn and oscillations with a period of 18 h or less in DD. To enable *TOC1* activation sufficiently early in the day in the double mutant, we required that *Y* transcription peaked sharply at dawn in the double mutant.

The 20 parameter sets with the lowest costs (which allowed the model to best fit the specified criteria) all simulated similar gene expression profiles in WT and *cca1;lhy* backgrounds (data not shown). An optimal parameter set was chosen from these 20 by comparing the simulated rhythms to experimental data that were not included in the cost function (see Results).

The equations were solved using MATLAB (Mathworks, Cambridge, UK). Parameter optimisation was carried out (Locke *et al*, 2005) by compiling MATLAB code into C and running the code on a task farm computer consisting of 62 × 2.6 GHz Xeon CPUs. We have developed a user-friendly interface, Circadian Modelling, to allow simulations using this and other circadian models, without MATLAB. This software and files for our final model are available online (Brown, 2004b).

Supplementary information

Supplementary information are available at the *Molecular Systems Biology* website (www.nature.com/msb).

Acknowledgements

We are grateful to OE Biringen-Akman, D Salazar, JA Langdale, CD Westbrook and DA Rand for useful discussions, and to N Shariff for technical assistance. JCWL was supported by a postgraduate studentship from the Gatsby Charitable Foundation; MMS was supported by a postgraduate studentship from BBSRC; LKB was supported by an EMBO postdoctoral fellowship; experimental work was funded by grants G15231 and G19886 from BBSRC to AJM. Computer facilities were provided by the Centre for Scientific Computing at the University of Warwick.

References

Alabadi D, Oyama T, Yanovsky MJ, Harmon FG, Mas P, Kay SA (2001) Reciprocal regulation between *TOC1* and *LHY/CCA1* within the *Arabidopsis* circadian clock. *Science* **293**: 880–883
Alabadi D, Yanovsky MJ, Mas P, Harmer SL, Kay SA (2002) Critical role for *CCA1* and *LHY* in maintaining circadian rhythmicity in *Arabidopsis*. *Curr Biol* **12**: 757–761
Brown KS, Sethna JP (2003) Statistical mechanical approaches to models with many poorly known parameters. *Phys Rev E Stat Nonlinear Soft Matter Phys* **68**: 021904
Brown PE (2004a) Biological Rhythms Analysis Software System <http://www.amillar.org/Downloads.html>
Brown PE (2004b) Circadian Modelling <http://www.amillar.org/Downloads.html>

Covington MF, Panda S, Liu XL, Strayer CA, Wagner DR, Kay SA (2001) ELF3 modulates resetting of the circadian clock in *Arabidopsis*. *Plant Cell* **13**: 1305–1315
Doyle MR, Davis SJ, Bastow RM, McWatters HG, Kozma-Bognar L, Nagy F, Millar AJ, Amasino RM (2002) The ELF4 gene controls circadian rhythms and flowering time in *Arabidopsis thaliana*. *Nature* **419**: 74–77
Dunlap JC (1999) Molecular bases for circadian clocks. *Cell* **96**: 271–290
Eriksson ME, Millar AJ (2003) The circadian clock. A plant's best friend in a spinning world. *Plant Physiol* **132**: 732–738
Fankhauser C, Staiger D (2002) Photoreceptors in *Arabidopsis thaliana*: light perception, signal transduction and entrainment of the endogenous clock. *Planta* **216**: 1–16
Farre EM, Harmer SL, Harmon FG, Yanovsky MJ, Kay SA (2005) Overlapping and distinct roles of PRR7 and PRR9 in the *Arabidopsis* circadian clock. *Curr Biol* **15**: 47–54
Fleissner G, Fleissner G (1992) Feedback loops in the circadian system. *Disc Neurosci* **8**: 79–84
Forger DB, Peskin CS (2003) A detailed predictive model of the mammalian circadian clock. *Proc Natl Acad Sci USA* **100**: 14806–14811
Fowler S, Lee K, Onouchi H, Samach A, Richardson K, Coupland G, Putterill J (1999) *GIGANTEA*: a circadian clock-controlled gene that regulates photoperiodic flowering in *Arabidopsis* and encodes a protein with several possible membrane-spanning domains. *EMBO J* **18**: 4679–4688
Glossop NRJ, Lyons LC, Hardin PE (1999) Interlocked feedback loops within the *Drosophila* circadian oscillator. *Science* **286**: 766–768
Green RM, Tobin EM (1999) Loss of the circadian clock-associated protein I in *Arabidopsis* results in altered clock-regulated gene expression. *Proc Natl Acad Sci USA* **96**: 4176–4179
Hall A, Bastow RM, Davis SJ, Hanano S, McWatters HG, Hibberd V, Doyle MR, Sung S, Halliday KJ, Amasino RM, Millar AJ (2003) The TIME FOR COFFEE gene maintains the amplitude and timing of *Arabidopsis* circadian clocks. *Plant Cell* **15**: 2719–2729
Harmer SL, Hogenesch JB, Straume M, Chang HS, Han B, Zhu T, Wang X, Kreps JA, Kay SA (2000) Orchestrated transcription of key pathways in *Arabidopsis* by the circadian clock. *Science* **290**: 2110–2113
Jewett ME, Forger DB, Kronauer RE (1999) Revised limit cycle oscillator model of human circadian pacemaker. *J Biol Rhythms* **14**: 493–499
Kim JY, Song HR, Taylor BL, Carre IA (2003) Light-regulated translation mediates gated induction of the *Arabidopsis* clock protein LHY. *EMBO J* **22**: 935–944
Lee K, Loros JJ, Dunlap JC (2000) Interconnected feedback loops in the *Neurospora* circadian system. *Science* **289**: 107–110
Leloup JC, Goldbeter A (2003) Toward a detailed computational model for the mammalian circadian clock. *Proc Natl Acad Sci USA* **100**: 7051–7056
Leloup JC, Gonze D, Goldbeter A (1999) Limit cycle models for circadian rhythms based on transcriptional regulation in *Drosophila* and *Neurospora*. *J Biol Rhythms* **14**: 433–448
Locke JCW, Millar AJ, Turner MS (2005) Modelling genetic networks with noisy and varied experimental data: the circadian clock in *Arabidopsis thaliana*. *J Theor Biol* **234**: 383–393
Makino S, Kiba T, Imamura A, Hanaki N, Nakamura A, Suzuki T, Taniguchi M, Ueguchi C, Sugiyama T, Mizuno T (2000) Genes encoding pseudo-response regulators: insight into His-to-Asp phosphorelay and circadian rhythm in *Arabidopsis thaliana*. *Plant Cell Physiol* **41**: 791–803
Makino S, Matsushika A, Kojima M, Oda Y, Mizuno T (2001) Light response of the circadian waves of the APRR1/TOC1 quintet: when does the quintet start singing rhythmically in *Arabidopsis*? *Plant Cell Physiol* **42**: 334–339
Makino S, Matsushika A, Kojima M, Yamashino T, Mizuno T (2002) The APRR1/TOC1 quintet implicated in circadian rhythms

- of *Arabidopsis thaliana*: I. Characterization with APRR1-overexpressing plants. *Plant Cell Physiol* **43**: 58–69
- Martinez-Garcia JF, Huq E, Quail PH (2000) Direct targeting of light signals to a promoter element-bound transcription factor. *Science* **288**: 859–863
- Mas P, Alabadi D, Yanovsky MJ, Oyama T, Kay SA (2003a) Dual role of TOC1 in the control of circadian and photomorphogenic responses in *Arabidopsis*. *Plant Cell* **15**: 223–236
- Mas P, Kim WY, Somers DE, Kay SA (2003b) Targeted degradation of TOC1 by ZTL modulates circadian function in *Arabidopsis thaliana*. *Nature* **426**: 567–570
- McWatters HG, Bastow RM, Hall A, Millar AJ (2000) The *ELF3 zeitnehmer* regulates light signalling to the circadian clock. *Nature* **408**: 716–720
- Millar AJ (2003) A suite of photoreceptors entrains the plant circadian clock. *J Biol Rhythms* **18**: 217–226
- Millar AJ, Kay SA (1996) Integration of circadian and phototransduction pathways in the network controlling *CAB* gene transcription in *Arabidopsis*. *Proc Natl Acad Sci USA* **93**: 15491–15496
- Mizoguchi T, Wheatley K, Hanzawa Y, Wright L, Mizoguchi M, Song HR, Carre IA, Coupland G (2002) LHY and CCA1 are partially redundant genes required to maintain circadian rhythms in *Arabidopsis*. *Dev Cell* **2**: 629–641
- Park DH, Somers DE, Kim YS, Choy YH, Lim HK, Soh MS, Kim HJ, Kay SA, Nam HG (1999) Control of circadian rhythms and photoperiodic flowering by the *Arabidopsis GIGANTEA* gene. *Science* **285**: 1579–1582
- Plautz JD, Straume M, Stanewsky R, Jamison CF, Brandes C, Dowse HB, Hall JC, Kay SA (1997) Quantitative analysis of *Drosophila period* gene transcription in living animals. *J Biol Rhythms* **12**: 204–217
- Rand DA, Shulgin BV, Salazar D, Millar AJ (2004) Design principles underlying circadian clocks. *Interface* **1**: 119–130
- Roden LC, Song HR, Jackson S, Morris K, Carre IA (2002) Floral responses to photoperiod are correlated with the timing of rhythmic expression relative to dawn and dusk in *Arabidopsis*. *Proc Natl Acad Sci USA* **99**: 13313–13318
- Roenneberg T, Merrow M (2002) Life before the clock: modeling circadian evolution. *J Biol Rhythms* **17**: 495–505
- Ruoff P, Behzadi A, Hauglid M, Vinsjevik M, Havas H (2000) ph homeostasis of the circadian sporulation rhythm in clock mutants of *Neurospora crassa*. *Chronobiol Int* **17**: 733–750
- Ruoff P, Vinsjevik M, Monnerjahn C, Rensing L (2001) The Goodwin model: simulating the effect of light pulses on the circadian sporulation rhythm of *Neurospora crassa*. *J Theor Biol* **209**: 29–42
- Salome PA, McClung CR (2004) The *Arabidopsis thaliana* clock. *J Biol Rhythms* **19**: 425–435
- Schaffer R, Ramsay N, Samach A, Corden S, Putterill J, Carre IA, Coupland G (1998) The late elongated hypocotyl mutation of *Arabidopsis* disrupts circadian rhythms and the photoperiodic control of flowering. *Cell* **93**: 1219–1229
- Smolen P, Hardin PE, Lo BS, Baxter DA, Byrne JH (2004) Simulation of *Drosophila* circadian oscillations, mutations, and light responses by a model with VRI, PDP-1, and CLK. *Biophys J* **86**: 2786–2802
- Somers DE, Kim WY, Geng R (2004) The F-box protein ZEITLUPE confers dosage-dependent control on the circadian clock, photomorphogenesis, and flowering time. *Plant Cell* **16**: 769–782
- Stelling J, Gilles ED, Doyle III FJ (2004) Robustness properties of circadian clock architectures. *Proc Natl Acad Sci USA* **101**: 13210–13215
- Strayer C, Oyama T, Schultz TF, Raman R, Somers DE, Mas P, Panda S, Kreps JA, Kay SA (2000) Cloning of the *Arabidopsis* clock gene TOC1, an autoregulatory response regulator homolog. *Science* **289**: 768–771
- Tyson JJ, Hong CI, Thron CD, Novak B (1999) A simple model of circadian rhythms based on dimerization and proteolysis of PER and TIM. *Biophys J* **77**: 2411–2417
- Ueda HR, Hagiwara M, Kitano H (2001) Robust oscillations within the interlocked feedback model of *Drosophila* circadian rhythm. *J Theor Biol* **210**: 401–406
- Wang ZY, Tobin EM (1998) Constitutive expression of the CIRCADIAN CLOCK ASSOCIATED 1 (CCA1) gene disrupts circadian rhythms and suppresses its own expression. *Cell* **93**: 1207–1217
- Yanovsky MJ, Kay SA (2002) Molecular basis of seasonal time measurement in *Arabidopsis*. *Nature* **419**: 308–312

Sup Figure 1: Network diagram for the single-loop *LHY/CCA1-TOC1* network. *TOC1* protein in the nucleus and light mediated by protein P (not shown) activate transcription of mRNA of *LHY*, which represents both *LHY* and *CCA1*. When *LHY* protein reaches the nucleus it represses *TOC1* mRNA transcription. Symbol convention as in Figure 1.

Sup Figure 2: Simulations of the *LHY/CCA1-TOC1-X* network. Left panel: simulated *TOC1* protein levels (dashed line), data from (Mas et al. 2003) (solid line). Maxima have been normalised to 1 for each trace. Right panel: Prediction of *X* mRNA (dotted line) and *X* protein levels (black line). In this and other supplementary figures, filled box above panel, dark interval; open or no box, light interval.

Sup Figure 3: Stability analysis of optimal parameter set in the interlocked feedback loop model. The period and amplitude of *TOC1* mRNA oscillations over 300h in LL are calculated for a 5% increase and decrease to each parameter value in turn. The circle represents the period and amplitude of the optimal parameter values.

Sup Figure 4: Simulations of the interlocked feedback loop network in LD12:12 and LL. Left panel: mRNA levels for WT in LD12:12 then LL. *LHY* mRNA level peaks at dawn (dotted line) and *TOC1* mRNA level (solid line) at dusk in LD cycles. Period is 25h in LL. Right panel: mRNA levels for *cca1;lhy* double mutant in LD12:12 then LL. *TOC1* mRNA peaks in the middle of the day and oscillates with an 18h period in LL, as seen experimentally in Fig 2.

Sup Figure 5: Effects of altered photoperiod on circadian rhythms. Simulations using the interlocked feedback network (dashed line), compared to data (solid line), under LD16:8 (upper panels) and LD8:16 (lower panels). *CCR2* mRNA data from (Roden et al. 2002) is used as a late evening marker to compare to simulations of *TOC1* mRNA (left-hand panels). *LHY* mRNA levels are from (Yanovsky & Kay 2002), highest value of data and simulation is set to 1 (right-hand panels).

Sup Figure 6: Effects of partial *y* loss-of-function in the interlocked feedback network. Simulation of *LHY* mRNA in WT (dashed line) and simulated *gi* mutant (solid line), simulated by halving the *Y* mRNA translation rate compared to WT.

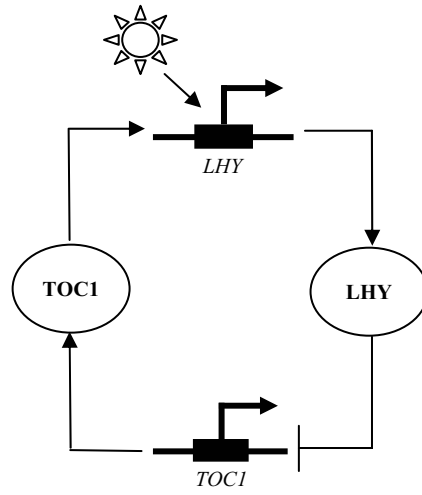
Sup Table 1: Optimal parameter values for *LHY/CCA1-TOC1-X* network

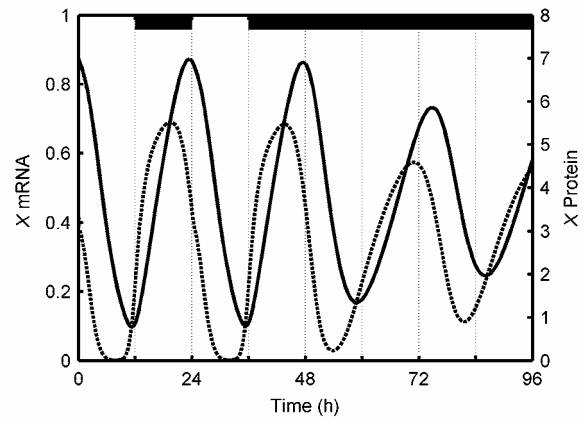
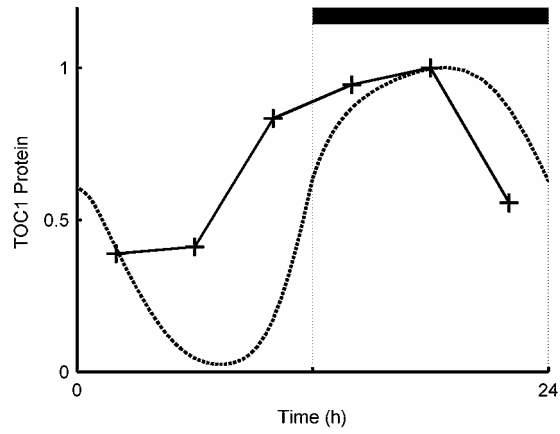
Sup. Table 2: Comparison of models: period estimates of the 3 models developed for the Arabidopsis circadian clock network are compared to experimental data. The simulation estimates are the average period over 300h in DD, for WT, *cca1* single mutant, and *cca1;lhy* double mutant. Experimental data for WT and *cca1* mutant periods from (Alabadi et al. 2002), *cca1;lhy* data from Fig 2.

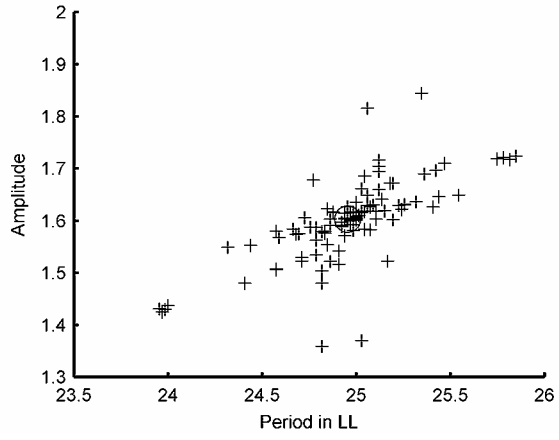
Sup Table 3: Optimal parameter values for interlocked feedback loop network

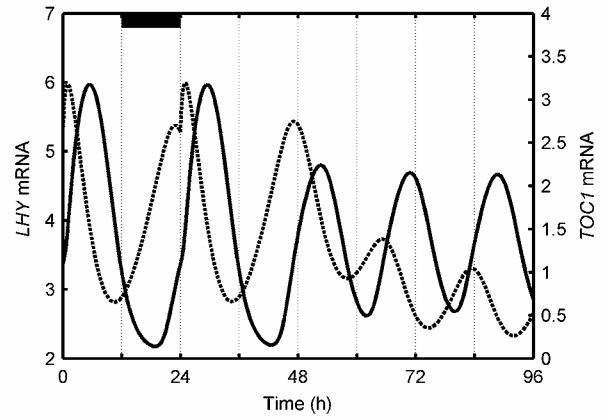
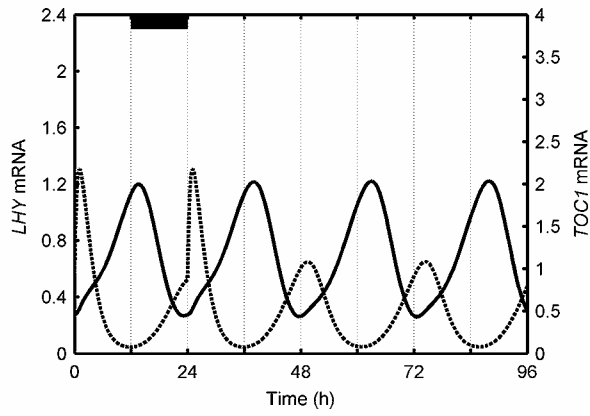
References:

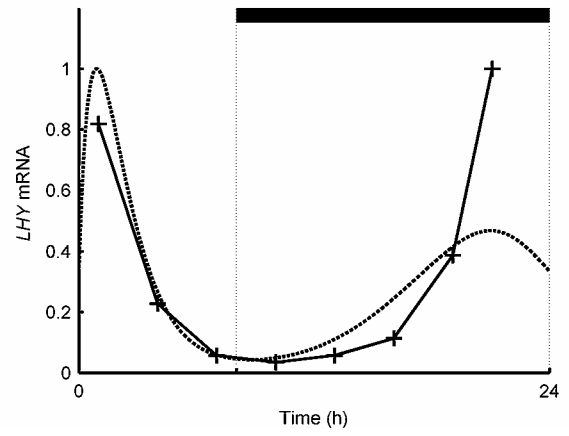
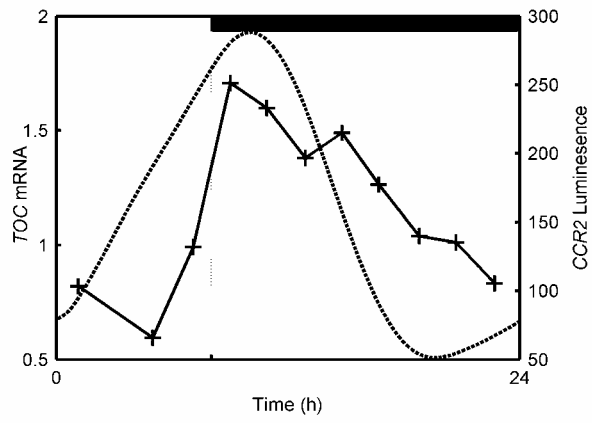
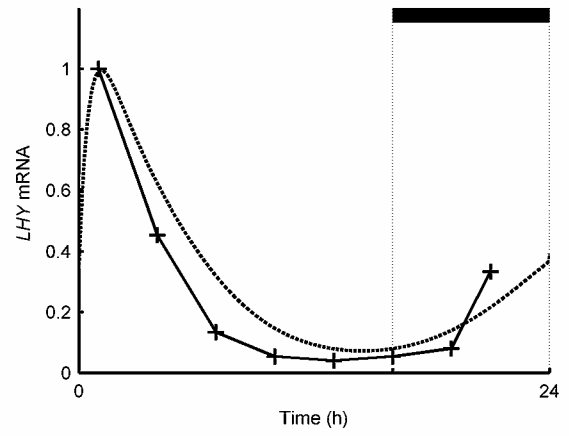
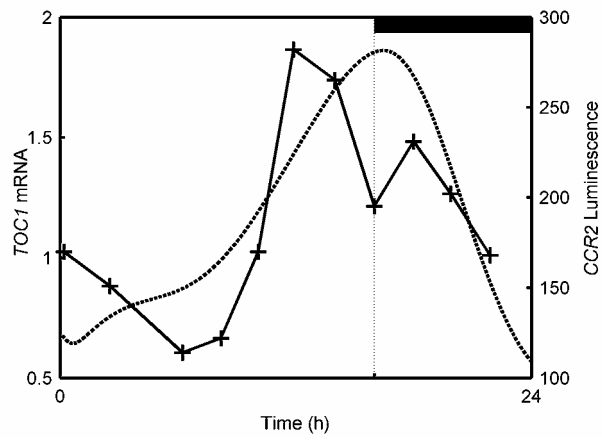
- Alabadi, D., Yanovsky, M. J., Mas, P., Harmer, S. L. & Kay, S. A. 2002 Critical role for CCA1 and LHY in maintaining circadian rhythmicity in Arabidopsis. *Curr Biol* **12**, 757-61.
- Mas, P., Kim, W. Y., Somers, D. E. & Kay, S. A. 2003 Targeted degradation of TOC1 by ZTL modulates circadian function in Arabidopsis thaliana. *Nature* **426**, 567-70.
- Roden, L. C., Song, H. R., Jackson, S., Morris, K. & Carre, I. A. 2002 Floral responses to photoperiod are correlated with the timing of rhythmic expression relative to dawn and dusk in Arabidopsis. *Proc Natl Acad Sci U S A* **99**, 13313-8.
- Yanovsky, M. J. & Kay, S. A. 2002 Molecular basis of seasonal time measurement in Arabidopsis. *Nature* **419**, 308-12.

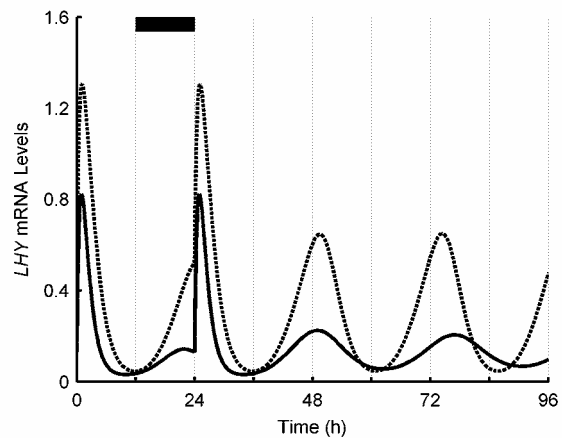












Parameter values for LHY/CCA1-TOC1-X Network			
Parameter Name	Parameter Value	Parameter Description	Dimensions
q1	12.2286	Coupling constant of light activation of LHY transcription	1/h
n1	9.4424	Maximum light-independent LHY transcription rate	nM/h
a	2	Hill coefficient of activation by X	
g1	2.0947	Constant of activation by protein X	nM
m1	8.0496	Maximum rate of LHY mRNA degradation	nM/h
k1	3.9155	Michaelis constant of LHY mRNA degradation	nM
p1	4.0188	Rate constant of LHY mRNA translation	1/h
r1	10.6578	Rate constant of LHY transport into nucleus	1/h
r2	1.0993	Rate constant of LHY transport out of nucleus	1/h
m2	2.1267	Maximum rate of cytoplasmic LHY degradation	nM/h
k2	0.2511	Michaelis constant of cytoplasmic LHY degradation	nM
m3	3.7925	Maximum rate of nuclear LHY degradation	nM/h
k3	8.4915	Michaelis constant of nuclear LHY degradation	nM
n2	3.4691	Maximum light-independent TOC1 transcription rate	nM/h
n3	1.2238	Maximum of light dependent activation of TOC1 transcription	1/h
b	2	Hill coefficient of repression by protein LHY	
g2	1.3859	Constant of repression by protein LHY	nM
m4	7.1075	Maximum rate of TOC1 mRNA degradation	nM/h
k4	2.2424	Michaelis constant of TOC1 mRNA degradation	nM
p2	2.1535	Rate constant of TOC1 mRNA translation	1/h
r3	0.6876	Rate constant of TOC1 movement into nucleus	1/h
r4	4.1674	Rate constant of TOC1 movement out of nucleus	1/h
m5	1.5743	Maximum rate of light dependent cytoplasmic TOC1 degradation	nM/h
m6	2.5529	Maximum rate of light independent cytoplasmic TOC1 degradation	nM/h
k5	1.8972	Michaelis constant of cytoplasmic TOC1 degradation	nM
m7	0.5879	Maximum rate of light dependent nuclear TOC1 degradation	nM/h
m8	0.9016	Maximum rate of light independent nuclear TOC1 degradation	nM/h
k6	2.6877	Michaelis constant of nuclear TOC1 degradation	nM
n4	2.6891	Maximum transcription rate of X mRNA	nM/h
c	2	Hill coefficient of activation by TOC1	
g3	1.9160	Constant of activation by TOC1	nM
m9	5.4578	Maximum rate of degradation of protein X mRNA	nM/h
k7	1.9433	Michaelis constant of protein X mRNA degradation	nM

Locke et al, Sup Table 1
(Continued)

Parameter Name	Parameter Value	Parameter Description	Dimensions
p3	2.4201	Rate constant of X mRNA translation	1/h
r5	2.0076	Rate constant of protein X movement into nucleus	1/h
r6	20.0848	Rate constant of protein X movement out of nucleus	1/h
m10	2.1119	Maximum rate of degradation of cytoplasmic protein X	nM/h
k8	5.2738	Michaelis constant of cytoplasmic protein X degradation	nM
m11	2.1795	Maximum rate of degradation of nuclear protein X	nM/h
k9	18.1832	Michaelis constant of nuclear protein X degradation	nM
p4	0.5	Light dependent production of protein P	nM/h
q2	1.0000	Coupling constant of light activation of protein P degradation	1/h
m12	1.2000	Maximum rate of protein P degradation	nM/h
k10	1.2000	Michaelis constant of protein P degradation	nM

	WT period (h)	<i>cca1</i> Single mutant (h)	<i>cca1/lhy</i> mutant (h)
Experimental data (± 1 S.E.M)	26.6 (± 0.2)	25.4 (± 0.2)	18.5 (± 0.3)
Interlocked Feedback Model	25.9	25.5	17.0
LHY/CCA1-TOC1-X single loop model	25.9	29.5	Arrhythmic
LHY/CCA1-TOC1 single loop model	25.0	29.2	Arrhythmic

Parameter values for interlocked feedback loop network			
Parameter Name	Parameter Value	Parameter Description	Dimensions
q1	2.4514	Coupling constant of light activation of LHY transcription	1/h
n1	5.1694	Maximum light-independent LHY transcription rate	nM/h
a	3.3064	Hill coefficient of activation by protein X	
g1	0.8767	Constant of activation by protein X	nM
m1	1.5283	Maximum rate of LHY mRNA degradation	nM/h
k1	1.8170	Michaelis constant of LHY mRNA degradation	nM
p1	0.8295	Rate constant of LHY mRNA translation	1/h
r1	16.8363	Rate constant of LHY transport into nucleus	1/h
r2	0.1687	Rate constant of LHY transport out of nucleus	1/h
m2	20.4400	Maximum rate of cytoplasmic LHY degradation	nM/h
k2	1.5644	Michaelis constant of cytoplasmic LHY degradation	nM
m3	3.6888	Maximum rate of nuclear LHY degradation	nM/h
k3	1.2765	Michaelis constant of nuclear LHY degradation	nM
n2	3.0087	Maximum TOC1 transcription rate	nM/h
b	1.0258	Hill coefficient of activation by protein Y	
g2	0.0368	Constant of activation by protein Y	nM
g3	0.2658	Constant of repression by LHY	nM
c	1.0258	Hill coefficient of repression by LHY	
m4	3.8231	Maximum rate of TOC mRNA degradation	nM/h
k4	2.5734	Michaelis constant of TOC mRNA degradation	nM
p2	4.3240	Rate constant of TOC1 mRNA translation	1/h
r3	0.3166	Rate constant of TOC1 movement into nucleus	1/h
r4	2.1509	Rate constant of TOC1 movement out of nucleus	1/h
m5	0.0013	Maximum rate of light dependent cytoplasmic TOC1 degradation	nM/h
m6	3.1741	Maximum rate of light independent cytoplasmic TOC1 degradation	nM/h
k5	2.7454	Michaelis constant of cytoplasmic TOC1 degradation	nM
m7	0.0492	Maximum rate of light dependent nuclear TOC1 degradation	nM/h
m8	4.0424	Maximum rate of light independent nuclear TOC1 degradation	nM/h
k6	0.4033	Michaelis constant of nuclear TOC1 degradation	nM
n3	0.2431	Maximum transcription rate of protein X	nM/h
d	1.4422	Hill coefficient of activation by TOC1	

Locke et al, Sup Table 3
(Continued)

Parameter Name	Parameter Value	Parameter Description	Dimensions
g4	0.5388	Constant of activation by TOC1	nM
m9	10.1132	Maximum rate of degradation of protein X mRNA	nM/h
k7	6.5585	Michaelis constant of protein X mRNA degradation	nM
p3	2.1470	Rate constant of X mRNA translation	1/h
r5	1.0352	Rate constant of protein X movement into nucleus	1/h
r6	3.3017	Rate constant of protein X movement out of nucleus	1/h
m10	0.2179	Maximum rate of degradation of cytoplasmic protein X	nM/h
k8	0.6632	Michaelis constant of cytoplasmic protein X degradation	nM
m11	3.3442	Maximum rate of degradation of nuclear protein X	nM/h
k9	17.1111	Michaelis constant of nuclear protein X degradation	nM
q2	2.4017	Coupling constant of light activation of Y mRNA transcription	1/h
n4	0.0857	Light dependent component of Y transcription	nM/h
n5	0.1649	Light independent component of Y transcription	nM/h
g5	1.1780	Constant of repression by TOC1	nM
g6	0.0645	Constant of repression by LHY	nM
e	3.6064	Hill coefficient of repression by TOC1	
f	1.0237	Hill coefficient of repression by LHY	
m12	4.2970	Maximum rate of degradation of protein Y mRNA	nM/h
k10	1.7303	Michaelis constant of protein Y mRNA degradation	nM
p4	0.2485	Rate constant of Y mRNA translation	1/h
r7	2.2123	Rate constant of protein Y movement into nucleus	1/h
r8	0.2002	Rate constant of protein Y movement out of nucleus	1/h
m13	0.1347	Maximum rate of degradation of cytoplasmic protein Y	nM/h
k11	1.8258	Michaelis constant of cytoplasmic protein Y degradation	nM
m14	0.6114	Maximum rate of degradation of nuclear protein Y	nM/h
k12	1.8066	Michaelis constant of nuclear protein Y degradation	nM
p5	0.5000	Light dependent production of protein P	nM/h
k13	1.2000	Michaelis constant of protein P degradation	nM
m15	1.2000	Maximum rate of protein P degradation	nM/h
q3	1.0000	Coupling constant of light activation of protein P degradation	1/h

1 Supplementary Text

1.1 Model One: *LHY/CCA1-TOC1-X Network*

The first network modelled (Fig 1) includes two extra components compared to the *LHY/CCA1-TOC1* network modelled in (Locke et al., 2005); An extra gene, called *X*, was added to the pathway, and a constant light activation term was added to *TOC1*. As in previous clock models (Locke et al., 2005; Leloup et al., 1999; Leloup and Goldbeter, 2003; Ueda et al., 2001; Kurosawa and Iwasa, 2002; Kurosawa et al., 2002) Michaelis-Menten kinetics were used to describe enzyme mediated degradation of proteins, and Hill functions were used to describe the transcriptional activation term of the mRNA for *LHY* and *TOC1*. We use the cytosolic and nuclear pools of our model proteins to represent all the processes between the accumulation of an mRNA and the regulation of the next gene in the network by an active form of the cognate protein. There is some evidence that Michaelis-Menten kinetics may not be an accurate approximation of processes in higher organisms, and other clock models (Forger and Peskin, 2003) include additional processes, such as mRNA export from the nucleus, but there is currently no data to specify their dynamics in plants. The converse approach is to combine all intermediate steps as a time delay between the synthesis of RNA and active protein. This aids intuitive understanding by reducing the number of model components, so simplified versions of our models will be described elsewhere (JCL, MST and AJM, unpublished results). Given that the time delays can hamper subsequent mathematical analysis, we present the more detailed models here.

As *LHY* and *CCA1* are indistinguishable for our purposes, we retain only one gene, *LHY*, in our model. Quantitative differences in *LHY* and *CCA1* regulation have sometimes been reported (Mizoguchi et al., 2002), though their qualitative behaviour is very similar. Differences in the response to *LHY*

and *CCA1* overexpression might occur but current data (Fowler et al., 1999) include potentially confounding effects of overexpression level, genetic background, and developmental stage. Combining *LHY* and *CCA1* genes removes 16 parameters and 3 equations from the model, which can be included when they are informed by further data.

We took the following as our mathematical model for the central circadian network: a LHY-TOC1-X feedback loop which involves the cellular concentrations $c_i^{(j)}(t)$ of the products of the i^{th} gene ($i = L$ labels LHY, $i = T$ labels TOC1, $i = X$ labels X) where $j = m, c, n$ denotes that it is the corresponding mRNA, or protein in the cytoplasm or nucleus respectively.

$$\frac{dc_L^{(m)}}{dt} = q_1 c_P^{(n)} \Theta(t) + \frac{n_1 c_X^{(n)a}}{g_1^a + c_X^{(n)a}} - \frac{m_1 c_L^{(m)}}{k_1 + c_L^{(m)}} \quad (1)$$

$$\frac{dc_L^{(c)}}{dt} = p_1 c_L^{(m)} - r_1 c_L^{(c)} + r_2 c_L^{(n)} - \frac{m_2 c_L^{(c)}}{k_2 + c_L^{(c)}} \quad (2)$$

$$\frac{dc_L^{(n)}}{dt} = r_1 c_L^{(c)} - r_2 c_L^{(n)} - \frac{m_3 c_L^{(n)}}{k_3 + c_L^{(n)}} \quad (3)$$

$$\frac{dc_T^{(m)}}{dt} = \frac{(n_2 + \Theta(t) n_3) g_2^b}{g_2^b + c_L^{(n)b}} - \frac{m_4 c_T^{(m)}}{k_4 + c_T^{(m)}} \quad (4)$$

$$\frac{dc_T^{(c)}}{dt} = p_2 c_T^{(m)} - r_3 c_T^{(c)} + r_4 c_T^{(n)} - ((1 - \Theta(t)) m_5 + m_6) \frac{c_T^{(c)}}{k_5 + c_T^{(c)}} \quad (5)$$

$$\frac{dc_T^{(n)}}{dt} = r_3 c_T^{(c)} - r_4 c_T^{(n)} - ((1 - \Theta(t)) m_7 + m_8) \frac{c_T^{(n)}}{k_6 + c_T^{(n)}} \quad (6)$$

$$\frac{dc_X^{(m)}}{dt} = \frac{n_4 c_T^{(n)}}{g_3^c + c_T^{(n)c}} - \frac{m_9 c_X^{(m)}}{k_7 + c_X^{(m)}} \quad (7)$$

$$\frac{dc_X^{(c)}}{dt} = p_3 c_X^{(m)} - r_5 c_X^{(c)} + r_6 c_X^{(n)} - \frac{m_{10} c_X^{(c)}}{k_8 + c_X^{(c)}} \quad (8)$$

$$\frac{dc_X^{(n)}}{dt} = r_5 c_X^{(c)} - r_6 c_X^{(n)} - \frac{m_{11} c_X^{(n)}}{k_9 + c_X^{(n)}} \quad (9)$$

$$\frac{dc_P^{(n)}}{dt} = (1 - \Theta) p_4 - \frac{m_{12} c_P^{(n)}}{k_{10} + c_P^{(n)}} - q_2 \Theta c_P^{(n)} \quad (10)$$

Here the various rate constants n_j , g_j etc parameterise transcription (n_j , g_j), degradation (m_j , k_j), translation (p_j), and the nuclear \leftrightarrow cytoplasmic protein transport (r_j). There is evidence that LHY and CCA1 proteins bind as a dimer to the promoter of *TOC1* (Daniel et al., 2004), and that there is only one active binding site on the *TOC1* promoter (Alabadi et al., 2001), so the Hill coefficient for *TOC1* inhibition by LHY protein, b , was set to 2. As there is no experimental evidence to support different values for the Hill coefficients a and c these were also set to 2. The acute light effect appears through the term $q_1 c_P^{(n)} \Theta(t)$. Light is known to give an acute, transient activation response for expression of *LHY* and *CCA1* (Kim et al., 2003; Kaczorowski and Quail, 2003; Doyle et al., 2003). This was modelled as in (Locke et al., 2005), using a simple mechanism involving an interaction of a light sensitive protein P, with concentration $c_P^{(n)}$ with the *LHY* gene promoter. $\Theta = 1$ when light is present, 0 otherwise. The values of the four parameters that appear in the equation for $c_P^{(n)}$ are chosen so as to give an acute light activation profile which is close to that observed in experiment. The essential features of Eq 10 are that P is produced only when light is absent and is degraded strongly when light is present.

A constant light activation term was added to X mRNA production, $\Theta(t) n_3$, and the effect of ZTL is modelled by the degradation terms for TOC1 in the cytoplasm and the nucleus, which are dark activated as suggested in (Mas et al., 2003).

1.2 Model Two: The interlocked feedback loop model

For the interlocked feedback loop model an extra loop is added to the network structure of the LHY/CCA1-TOC1-X circuit. Here a hypothetical gene Y activates *TOC1*, and TOC1 then feeds back to repress Y . The light input into this loop is moved from *TOC1* to Y as there is no evidence of light activation of

TOC1 (Makino et al., 2002). *Y* was allowed to be both acutely light activated, in the manner of *LHY*, so to explain the extremely light sensitive response seen experimentally in the PTC of the *cca1;lhyl* mutant (Figure 2), and to have a constant light activation term, to allow the clock to sense photoperiod.

We used a non-cooperative binding term for the activation and repression of *TOC1* by *Y* and *LHY* respectively, and for the repression of *Y* by *TOC1* and *LHY*. This means that *LHY* represses *TOC1* transcription irrespective of the levels of *Y*.

The Hill coefficients in the equations were allowed to vary between 1 and 4 in the optimisation procedure. In order to obtain a compromise between flexibility and overall number of free parameters the Hill coefficients of activation and repression of *TOC1* were set to the same value, i.e. $b = c$.

$$\frac{dc_L^{(m)}}{dt} = \Theta(t) q_1 c_P^{(n)} + \frac{n_1 c_X^{(n)a}}{g_1^a + c_X^{(n)a}} - \frac{m_1 c_L^{(m)}}{k_1 + c_L^{(m)}} \quad (11)$$

$$\frac{dc_L^{(c)}}{dt} = p_1 c_L^{(m)} - r_1 c_L^{(c)} + r_2 c_L^{(n)} - \frac{m_2 c_L^{(c)}}{k_2 + c_L^{(c)}} \quad (12)$$

$$\frac{dc_L^{(n)}}{dt} = r_1 c_L^{(c)} - r_2 c_L^{(n)} - \frac{m_3 c_L^{(n)}}{k_3 + c_L^{(n)}} \quad (13)$$

$$\frac{dc_T^{(m)}}{dt} = \left(\frac{n_2 c_Y^{(n)b}}{g_2^b + c_Y^{(n)b}} \right) \left(\frac{g_3^c}{g_3^c + c_L^{(n)c}} \right) - \frac{m_4 c_T^{(m)}}{k_4 + c_T^{(m)}} \quad (14)$$

$$\frac{dc_T^{(c)}}{dt} = p_2 c_T^{(m)} - r_3 c_T^{(c)} + r_4 c_T^{(n)} - ((1 - \Theta(t))m_5 + m_6) \frac{c_T^{(c)}}{k_5 + c_T^{(c)}} \quad (15)$$

$$\frac{dc_T^{(n)}}{dt} = r_3 c_T^{(c)} - r_4 c_T^{(n)} - ((1 - \Theta(t))m_7 + m_8) \frac{c_T^{(n)}}{k_6 + c_T^{(n)}} \quad (16)$$

$$\frac{dc_X^{(m)}}{dt} = \frac{n_3 c_T^{(n)d}}{g_4^d + c_T^{(n)d}} - \frac{m_9 c_X^{(m)}}{k_7 + c_X^{(m)}} \quad (17)$$

$$\frac{dc_X^{(c)}}{dt} = p_3 c_X^{(m)} - r_5 c_X^{(c)} + r_6 c_X^{(n)} - \frac{m_{10} c_X^{(c)}}{k_8 + c_X^{(c)}} \quad (18)$$

$$\frac{dc_X^{(n)}}{dt} = r_5 c_X^{(c)} - r_6 c_X^{(n)} - \frac{m_{11} c_X^{(n)}}{k_9 + c_X^{(n)}} \quad (19)$$

$$\frac{dc_Y^{(m)}}{dt} = \left(\Theta(t) q_2 c_P^{(n)} + \frac{(\Theta(t) n_4 + n_5) g_5^e}{g_5^e + c_T^{(n)e}} \right) \left(\frac{g_6^f}{g_6^f + c_L^{(n)f}} \right) - \frac{m_{12} c_Y^{(m)}}{k_{10} + c_Y^{(m)}} \quad (20)$$

$$\frac{dc_Y^{(c)}}{dt} = p_4 c_Y^{(m)} - r_7 c_Y^{(c)} + r_8 c_Y^{(n)} - \frac{m_{13} c_Y^{(c)}}{k_{11} + c_Y^{(c)}} \quad (21)$$

$$\frac{dc_Y^{(n)}}{dt} = r_7 c_Y^{(c)} - r_8 c_Y^{(n)} - \frac{m_{14} c_Y^{(n)}}{k_{12} + c_Y^{(n)}} \quad (22)$$

$$\frac{dc_P^{(n)}}{dt} = (1 - \Theta(t)) p_5 - \frac{m_{15} c_P^{(n)}}{k_{13} + c_P^{(n)}} - q_3 \Theta(t) c_P^{(n)} \quad (23)$$

1.3 Optimisation process

We follow the optimisation technique as described (Locke et al., 2005). We summarise the technique here, but for a full description please refer to (Locke et al., 2005). There is significant noise in the experimental data for the mRNA levels of the key genes in the clock of Arabidopsis, and very little data for protein abundance, making a direct fit to the data difficult. This motivated us to construct an empirical cost function designed to give a value for the goodness of fit of our solution to qualitative features that are consistent in the data.

We constructed our cost function Δ as a sum of terms that each quantify the agreement between our model and a qualitative experimental feature. Small values of the cost function correspond to a model (or set of parameter values) that give a good qualitative agreement with the corresponding experimental features. The weighting of each term in the cost function was chosen so that an acceptable error within the range of experimental variability would add on the order of 1 unit to the cost function. In order to evaluate the terms in the cost function we solved the equations numerically over 600 hours, 300 hours in 12 hour light 12 hour dark cycles (LD), followed by 300 hours in darkness

(DD) (the first 200 hours of the LD cycles of each solution are discarded as transitory). In order to find a set of optimal solutions for each network studied, the cost function was calculated for a cross section of parameter space chosen using a Sobol quasi-random number generator (Press et al., 1996). The best fifty solutions were then put through a further optimisation step using a simulated annealing routine (Brooks and Morgan, 1995).

For the LHY/CCA1-TOC1-X network the cost function is essentially the same as that used in (Locke et al., 2005). We reproduce here the description of the cost function from Appendix A of that paper. The cost function is given by:

$$\Delta = \delta_{\tau_d} + \delta_{\tau_d} + \delta_{\phi} + \delta_{c_L} + \delta_{\text{size}}. \quad (24)$$

Firstly,

$$\delta_{\tau_d} = \sum_{i=L,T} \langle (24 - \tau_i^{(m)})^2 / 0.15 \rangle_{ld} \quad (25)$$

Is the summed error in the period, τ , for *LHY* (L) and *TOC1* (T) mRNA levels in light:dark cycles (LD), where $\langle \rangle_{ld}$ gives the average over the cycles between $200 < t < 300$, and a “marginally acceptable” period difference of ≈ 25 mins contributes $O(1)$ to the cost function.

Secondly,

$$\delta_{\tau_d} = \sum_{i=L,T} \langle (25 - \tau_i^{(m)})^2 / f \rangle_d \quad (26)$$

where the average of $\langle \rangle_d$ is now over $300 < t < 600$ (DD). The biological evidence strongly indicates that the free running period of the clock is greater than 24 (Millar et al., 1995), probably about 25, but we have less confidence in assigning a precise value hence we adopt values of $f = 0.05$ if $\tau_i^{(m)} \leq 25$ and $f = 2$ if $\tau_i^{(m)} > 25$.

Thirdly,

$$\delta_\phi = \sum_{i=L,T} \left[\langle \Delta\Phi_i^2 \rangle_{ld} + \left(\frac{\sigma[c_i^{(m)}(t_p)]_{ld}}{0.05 \langle c_i^{(m)}(t_p) \rangle_{ld}} \right)^2 + \left(\frac{\sigma[\Delta\Phi_i]}{5/60} \right)^2 \right] + \delta_{ent} \quad (27)$$

The first term compares the mean difference in phase over the LD cycles, where $\Delta\Phi_i = \bar{\phi}_i - \phi_i$, ϕ_i is the phase (from dawn) of the RNA peak in the model and $\bar{\phi}_L = 1\text{h}$, $\bar{\phi}_T = 11\text{h}$ are the target phases of the peaks in $c_L^{(m)}$ and $c_T^{(m)}$ respectively. We assume a cost that is $O(1)$ for solutions that differ by an hour. The next two terms ascribe a cost of $O(1)$ for limit cycle solutions in LD cycles whose peak heights are within 5 percent, and whose variation in peak times is 5 minutes. $\sigma[\]_{ld}$ is the standard deviation for the cycles in LD. The term δ_{ent} checks that the solution is truly entrained to the light/dark cycle, i.e is not oscillating with the correct phase simply because of the initial conditions chosen, as follows: The solution is rerun for 75 hours, taking the solution at 202 hours and shifting it back 3 hours, i.e initialising the $t = 202$ solution as the $t = 199$ solution. The new phase of the second peak is compared to the original phase of the second peak. If the phase difference is still near 3 hours, then the solution is too weakly entrained, and the solution is pathological. The LD cycles have failed to phase shift the response. Hence δ_{ent} takes the form of $\log(0.5)/\log(\delta\phi/3)$, where $\delta\phi$ is the phase difference in hours between the shifted and original solution, and $\delta\phi/3$ is therefore the fraction of the imposed 3 hour phase shift remaining after 2 periods. The term $\log(0.5)$ gives the acceptable remaining phase difference of 1.5 hours for the second cycle, which results in an $O(1)$ contribution to the cost function.

Next,

$$\delta_{\text{size}} = \sum_{i=L,T} \left(\frac{1}{\langle \Delta c_i^{(m)} \rangle_{ld}} \right)^2 + \left(\frac{\tau_o}{\tau_e} \right)^2 \quad (28)$$

The first term costs for solutions in LD cycle with oscillation sizes, $(\Delta c_i^{(m)} =$

$c_i^{(m)_{max}} - c_i^{(m)_{min}}$), less than 1nm, and the second term checks that the oscillations do not decay too quickly when entering DD as follows: τ_o is a decay constant over the 300 hours in DD, $\tau_o = -300/\log((\Delta c_T^{(m)_{ld}} - \Delta c_T^{(m)_{d}})/\Delta c_T^{(m)_{ld}})$, and τ_e gives the acceptable decay constant, that *TOC1* oscillations size has dropped by 1/4 over 300 hours, $-300/\log(0.75)$.

Finally,

$$\begin{aligned} \delta_{c_L} = & \sum_{i=2,-2} \left\langle \left(\frac{2/3c_L^{(m)}(t_p)}{c_L^{(m)}(t_p) - c_L^{(m)}(t_p + i)} \right)^2 \right\rangle_{ld} + \dots \\ & \left\langle \left(\frac{0.05(c_L^{(m)}(t_p - 2) - c_L^{(m)}(t_m))}{c_L^{(m)}(t_m) - c_L^{(m)}(t_m + i)} \right)^2 \right\rangle_{ld} + 10 \left(\frac{\langle c_L^{(m)}(t_{pd}) \rangle_{ld}}{\langle c_L^{(m)}(t_{pl}) \rangle_{ld}} \right)^4 \end{aligned} \quad (29)$$

The first term checks that the *LHY* mRNA expression profile has a sharp peak in LD cycles, with an O(1) contribution if *LHY*'s expression level has dropped by 2/3 of its oscillation size within 2 hours before and after its peak of expression. The second term checks that *LHY* mRNA expression has a broad minimum, with an O(1) contribution if 2 hours before and after the minimum point *LHY*'s expression has only increased to 5 percent of the level 2 hours before *LHY*'s peak. The last term checks that the peak of *LHY* mRNA expression drops from LD into DD, as it loses its light activation. An additional cost term was added to shape fit the *TOC1* mRNA profile, as suggested in (Locke et al., 2005) in order to stop spurious solutions where *TOC1* mRNA expression is saturated, but this term was found to be unnecessary for optimising a network where *TOC1* is light activated, and was not used for further optimisations.

Throughout the implementation the cost function was ‘‘capped’’ at $\Delta_{\max} = 10^4$, such that $\Delta \rightarrow \text{Min}(10^4, \Delta)$.

As discussed in the computational methods, we added new terms to the cost function in order to optimise the interlocked feedback loop model to both WT

and *cca1;lhy* mutant data. The equations were re-solved with the translation rate of *LHY* reduced to a thousandth of its WT value in order to simulate the double mutant. The cost function now becomes

$$\Delta = \delta_{\tau_{ld}} + \delta_{\tau_d} + \delta_{\phi} + \delta_{c_L} + \delta_{\text{size}} + \delta_{\phi_d} + \delta_{\tau_{ld}}^{dm} + \delta_{\tau_d}^{dm} + \delta_{\phi}^{dm} + \delta_{c_Y}^{dm} + \delta_{\text{size}}^{dm} \quad (30)$$

where the label (*dm*) denotes the cost function for the *cca1;lhy* double mutant. One new WT cost function term δ_{ϕ_d} added represents a minor change to constrain an appropriate phase difference between the peak levels of *LHY* and *TOC1* mRNA, $\Delta\Phi_d = \phi_T - \phi_L$ (modulo half the period), with a characteristic prefactor of 10h. This term makes no discernable difference to the cost function when applied to the optimised one loop models. See term below:

$$\delta_{\phi_d} = (10/\Delta\Phi_d)^2 \quad (31)$$

δ_{size} was also altered slightly in order to ensure both *LHY* mRNA and *TOC1* mRNA oscillations do not decay too quickly when entering DD. This is necessary as in the interlocked feedback loop model *TOC1* mRNA levels can oscillate through *TOC1*'s feedback loop with *Y* whilst *LHY* mRNA levels are arrhythmic. δ_{size} becomes

$$\delta_{\text{size}} = \sum_{i=L,T} \left[\left(\frac{1}{\langle \Delta c_i^{(m)} \rangle_{ld}} \right)^2 + \left(\frac{\tau_o}{\tau_e} \right)^2 \right]. \quad (32)$$

The first term remains the same, and the second term is now summed over *LHY* (L) and *TOC1* (T). All the other WT cost function terms remain the same as for the one loop model optimisation.

Using the same methodology as for the WT terms, we define below the new

double mutant terms of the cost function. The first new term,

$$\delta_{\tau_{ld}}^{dm} = \sum_{i=Y,T} \langle (24 - \tau_i^{(m)})^2 / 0.15 \rangle_{ld} \quad (33)$$

is the summed error in the period, τ , for Y (Y) and $TOC1$ (T) mRNA levels in LD cycles.

We penalise solutions with a period of $TOC1$ greater than 18 hours in the dark. $\delta_{\tau_{ld}}^{(m)} = 0$ if the period is less than 18 hours, otherwise:

$$\delta_{\tau_d}^{dm} = \langle (18 - \tau_T^{(m)})^2 / 0.1 \rangle_d \quad (34)$$

Next,

$$\delta_{\phi}^{dm} = \sum_{i=Y,T} \left[\langle \Delta\Phi_i^2 \rangle_{ld} + (\sigma[\Delta\Phi_i])^2 \right] \quad (35)$$

The first term compares the mean difference in phase over the LD cycles, where $\Delta\Phi_i = \bar{\phi}_i - \phi_i$, ϕ_i is the phase (from dawn) of the RNA peak in the model and $\bar{\phi}_Y = 1h$, $\bar{\phi}_T = 5h$ are the target phases of the peaks in $c_Y^{(m)}$ and $c_T^{(m)}$ respectively. The second term describes a cost of $O(1)$ for solutions whose variations in peak phases are 1h. Next,

$$\delta_{size}^{dm} = \sum_{i=Y,T} \left(\frac{1}{\langle \Delta c_i^{(m)} \rangle_{ld}} \right)^2 \quad (36)$$

This term costs for solutions in LD cycle with oscillation sizes, $(\Delta c_i^{(m)} = c_{i \max}^{(m)} - c_{i \min}^{(m)})$, less than 1nm. Finally,

$$\delta_{c_Y}^{dm} = \sum_{i=2,-2} \left\langle \left(\frac{2/3 c_Y^{(m)}(t_p)}{c_Y^{(m)}(t_p) - c_Y^{(m)}(t_p + i)} \right)^2 \right\rangle_{ld} \quad (37)$$

The first term checks that the Y mRNA expression profile has a sharp peak

in LD cycles, with an $O(1)$ contribution if Y 's expression level has dropped by $2/3$ of its oscillation size within 2 hours before and after its peak of expression. As for the single loop optimisations, throughout the implementation the cost function was “capped” at $\Delta_{\max} = 10^4$, such that $\Delta \rightarrow \text{Min}(10^4, \Delta)$. The sum of the double mutant cost function terms was also capped at 10^3 .

References

- Alabadi, D., Oyama, T., Yanovsky, M. J., Harmon, F. G., Mas, P., Kay, S. A., 2001. Reciprocal regulation between TOC1 and LHY/CCA1 within the Arabidopsis circadian clock. *Science* 293, 880–883.
- Brooks, S. P., Morgan, B., 1995. Optimization using simulated annealing. *The Statistician* 44, 241–257.
- Daniel, X., Sugano, S., Tobin, E. M., 2004. CK2 phosphorylation of CCA1 is necessary for its circadian oscillator function in Arabidopsis. *Proc. Natl. Acad. Sci* 101, 3292–3297.
- Doyle, M. R., Davis, S. J., Bastow, R. M., McWatters, H. G., Kozma-Bognar, L., Nagy, F., Millar, A. J., Amasino, R., 2003. The ELF4 gene controls circadian rhythms and flowering time in Arabidopsis thaliana. *Nature* 424, 732–738.
- Forger, D. B., Peskin, C. S., 2003. A detailed predictive model of the mammalian clock. *Proc. Natl. Acad. Sci.* 100, 14806–14811.
- Fowler, S., Lee, K., Onouchi, H., Samach, A., Richardson, K., Morris, B., Coupland, G., Putterill, J., 1999. GIGANTEA: a circadian clock-controlled gene that regulates photoperiodic flowering in Arabidopsis and encodes a protein with several possible membrane-spanning domains. *The EMBO Journal* 18, 4679–4688.
- Kaczorowski, K. A., Quail, P. H., 2003. Arabidopsis PSEUDO-RESPONSE REGULATOR7 is a signaling intermediate in phytochrome-regulated seedling deetiolation and phasing of the circadian clock. *Plant Cell* 15, 2654–2665.
- Kim, J. Y., Song, H. R., Taylor, B. L., Carre, I. A., 2003. Light-regulated translation mediates gated induction of the Arabidopsis clock protein LHY. *EMBO J* 22, 935–944.
- Kurosawa, G., Iwasa, Y., 2002. Saturation of enzyme kinetics in circadian clock models. *J. Biol. Rhythms* 17, 568–577.
- Kurosawa, G., Mochizuki, A., Iwasa, Y., 2002. Comparative study of circadian clock models, in search of processes promoting oscillation. *J. Theor. Biol.* 216, 193–208., doi:10.1006/jtbi.2002.2546.

- Leloup, J. C., Goldbeter, A., 2003. Toward a detailed computational model for the mammalian circadian clock. *Proc. Natl. Acad. Sci* 100, 7051–7056.
- Leloup, J. C., Gonze, D., Goldbeter, A., 1999. Limit cycle models for circadian rhythms based on transcriptional regulation in *Neurospora* and *Drosophila*. *J. Biol. Rhythms* 14, 433–448.
- Locke, J. C. W., Millar, A. J., Turner, M. S., 2005. Modelling genetic networks with noisy and varied data: The circadian clock in *Arabidopsis thaliana*. *J Theor. Biology* 234, 383–393.
- Makino, S., Matsushika, A., Kojima, M., Yamashino, T., Mizuno, T., 2002. The APRR1/TOC1 quintet implicated in circadian rhythms of *Arabidopsis thaliana*: 1. characterization with APRR1-overexpressing plants. *Plant Cell Physiol* 43, 58–69.
- Mas, P., Kim, W. Y., Somers, D. E., Kay, S. A., 2003. Targeted degradation of TOC1 by ZTL modulates circadian function in *Arabidopsis thaliana*. *Nature* 426, 567–570.
- Millar, A. J., Straume, M., Chory, J., Chua, N. H., Kay, S. A., 1995. The regulation of circadian period by phototransduction pathways in *Arabidopsis*. *Science* 267, 1163–1166.
- Mizoguchi, T., Wheatley, K., Hanzawa, Y., Wright, L., Mizoguchi, M., Song, H. R., Carre, I. A., Coupland, G., 2002. LHY and CCA1 are partially redundant genes required to maintain circadian rhythms in *Arabidopsis*. *Dev Cell* 2, 629–641.
- Press, W. H., Teukolsky, S. A., Vetterling, W. T., Flannery, B. P., 1996. *Numerical Recipes in C: The Art of Scientific Computing*. Cambridge, Cambridge.
- Ueda, H. R., Hagiwara, M., Kitano, H., 2001. Robust oscillations within the interlocked feedback model of *drosophila* circadian rhythm. *J. Theor. Biol* 210, 401–406., doi:10.1006/jtbi.2000.2226.